AFCRL- 72-0128

FIELD ALIGNED E- AND F-LAYER BACKSCATTER OBSERVATIONS

by

SUNANDA BASU

ROBERT L. VESPRINI

EMMANUEL COLLEGE
400 THE FENWAY
BOSTON, MASSACHUSETTS 02115

Contract No. F19628-71-C-0250

Project No. 414L

Scientific Report No. 1

January 1972

Contract Monitor: Jules Aarons

Ionospheric Physics Laboratory

This research was supported by the
Electronics Systems Division.

Approved for public release; distribution unlimited.

Prepared for

AIR FORCE CAMBRIDGE RESEARCH LABORATORIES
AIR FORCE SYSTEMS COMMAND
UNITED STATES AIR FORCE
BEDFORD, MASSACHUSETTS 01730

Unclassified
Security Classification

DOCUMENT CONTROL DATA - R & D

(Security classification of title, body of abstract and indexing annotation must be entered when the overall report is classified)

1. ORIGINATING ACTIVITY (Corporate author)
Emmanuel College
400 The Fenway
Boston, Massachusetts 02115

2a. REPORT SECURITY CLASSIFICATION
Unclassified

2b. GROUP

3. REPORT TITLE
FIELD ALIGNED E- AND F-LAYER BACKSCATTER OBSERVATIONS

4. DESCRIPTIVE NOTES (Type of report and inclusive dates)
Scientific. Interim.

5. AUTHOR(S) (First name, middle initial, last name)
Sunanda Basu
Robert L. Vesprini

6. REPORT DATE	7a. TOTAL NO OF PAGES	7b. NO. OF REFS
January 1972	55	13

8a. CONTRACT OR GRANT NO
F19628-71-C-0250

8b. PROJECT, TASK, AND WORK UNIT NO.
414L N/A N/A

8c. DOD ELEMENT
12417F

8d. DOD SUBELEMENT 67414L

9a. ORIGINATOR'S REPORT NUMBER(S)
Scientific Report No. 1

9b. OTHER REPORT NO(S) (Any other numbers that may be assigned this report)
AFCRL-72-0128

10. DISTRIBUTION STATEMENT
A - Approved for public release; distribution unlimited.

11. SUPPLEMENTARY NOTES
This research was supported by the Electronics Systems Division

12. SPONSORING MILITARY ACTIVITY
Air Force Cambridge Research Laboratories(LI
L.G. Hanscom Field
Bedford, Massachusetts 01730

13. ABSTRACT

In a reanalysis of the HF (19MHz) backscatter data from Plum Island MA, the occurrence of field aligned echoes from the E and F layers, called FAE(E) and FAE(F) respectively, was studied in detail. FAE(E) during quiet magnetic conditions (K_{Fr}0-3) is a nighttime phenomenon with a definite maximum during the summer, when it is accompanied by groundscattered E_s. A weaker maximum is observed in the winter. Geomagnetic activity increases the occurrence of FAE(E) when no seasonal control is evident. During quiet magnetic conditions, FAE(F) are confined primarily to sunset hours. The equinoxes show more activity than the solstices, and the FAE(F) are generally accompanied by F-layer supported groundscatter echoes. FAE(F) shows a positive correlation with solar cycle. The incidence of FAE(F) increases monotonically with K_{Fr} until a threshold value is reached ($K_{Fr} \geq 4$), beyond which the depletion in the background ionization causes it to decrease, with complete cut-off for $K_{Fr} \geq 7$.

DD FORM NOV 1473

Unclassified
Security Classification

14 KEY WORDS	LINK A		LINK B		LINK C	
	ROLE	WT	ROLE	WT	ROLE	WT
Aurora						
Ionosphere						
Radar						

AFCRL- 72-0128

FIELD ALIGNED E- AND F-LAYER BACKSCATTER OBSERVATIONS

by

SUNANDA BASU

ROBERT L. VESPRINI

EMMANUEL COLLEGE
400 THE FENWAY
BOSTON, MASSACHUSETTS 02115

Contract No. F19628-71-C-0250

Project No. 414L

Scientific Report No. 1

January 1972

Contract Monitor: Jules Aarons

Ionospheric Physics Laboratory

This research was supported by the
Electronics Systems Division.

Prepared for

AIR FORCE CAMBRIDGE RESEARCH LABORATORIES
AIR FORCE SYSTEMS COMMAND
UNITED STATES AIR FORCE
BEDFORD, MASSACHUSETTS 01730

ABSTRACT

In a reanalysis of the HF (19 MHz) backscatter data from Plum Island MA, the occurrence of field aligned echoes from the E and F layers, called FAE(E) and FAE(F) respectively, was studied in detail. From this site, direct orthogonality with the magnetic field can be achieved only at E-layer heights, whereas refraction is necessary for the F layer. FAE(E) during quiet magnetic conditions (K_{Fr}0-3) is a nighttime phenomenon with a definite maximum during the summer, when it is accompanied by groundscattered E_s. A weaker maximum is observed in the winter. Geomagnetic activity increases the occurrence of FAE(E) when no seasonal control is evident. During quiet magnetic conditions, FAE(F) are confined primarily to sunset hours. The equinoxes show more activity than the solstices, and the FAE(F) are generally accompanied by F-layer supported groundscatter echoes. FAE(F) shows a positive correlation with solar cycle. The incidence of FAE(F) increases monotonically with K_{Fr} until a threshold value is reached ($K_{Fr}\geq 4$), beyond which the depletion in the background ionization causes it to decrease, with complete cut-off for $K_{Fr}\geq 7$.

In the next scientific report, the occurrence characteristics of various groundscattered echoes will be presented and these will be used to explain qualitatively the observed characteristics of FAE.

TABLE OF CONTENTS

LIST OF FIGURES

Figure

Figure

1. INTRODUCTION

A continuous series of fixed frequency oblique backscatter observations was conducted at the Plum Island site (42.63°N, 70.82°W) of the Sagamore Hill Radio Observatory between January 1961 and December 1965. The primary objective of this program was to study the field aligned irregularities in the ionization density at both E-layer and F-layer heights. These irregularities are responsible for the auroral clutter which affects the performance of HF, and even VHF and UHF, high latitude radars whose purpose is to detect and track aircraft and missiles (Leadabrand, 1964). A preliminary analysis of a part of this data has been presented by Malik and Aarons (1964) in which they noted the frequent occurrence of auroral echoes over a three year period. A more recent analysis of the data has been made by Aarons (1971).

Studies of radar echoes from field aligned irregularities have been made for many years. However, studies of the field aligned E-region irregularities (to be henceforth referred to as FAE(E)) have been more numerous as indicated in the review articles by Booker (1960), Chamberlain (1961) and Bowles (1964). This is primarily because it is possible to achieve direct orthogonality at E-layer heights from most mid-latitude and sub-auroral stations. The condition that the earth's magnetic field be perpendicular to the probing radar signal, also referred to as the aspect sensitivity requirement, is a necessary condition for sufficient backscatter to occur. Recent work (Bates, 1971) has shown that the intensity of the backscattered signal falls off 5-6 dB per degree off orthogonality.

The detection of field aligned F-region irregularities (FAE(F)) from most mid-latitude stations, however, will require sufficient refraction in the underlying layers to achieve orthogonality at F-layer heights. In order that the amount of refraction be adequate, frequencies in the HF range have to be used. The geometrical situation for the Plum Island site is shown in

Figures 1a and 1b. The aspect sensitivity requirements are directly met at 110 km, whereas the lowest propagation angle achieved at F-layer heights is 100° for straight line propagation. Thus the refraction in the underlying layers has to bend the ray by at least 10° to meet the orthogonality criterion at a height of 300 km. The interpretation of the F-layer echoes should thus be viewed in this context; namely, the absence of echoes need not necessarily mean the absence of irregularities but could be due to insufficient refraction, such as under nighttime conditions.

2. EQUIPMENT

The data used for this study were obtained from film records of a 19.39 MHz sounder located at Plum Island, Massachusetts (56° invariant latitude). A low powered 1 kw peak-power radar was used with a pulse length of 1 millisecond and a repetition frequency of 10/sec. The pulses were transmitted by a horizontal three-element Yagi antenna placed 0.6λ above ground and rotating at the rate of one revolution every eight minutes. The receiver band width was 1 kc. The resulting data were recorded on compressed time-scale film as well as on the range azimuth (PPI) type frames. The maximum range on the sweep was 3750 km taken in 750 km steps. Field aligned echoes, both FAE(E) and FAE(F), and sporadic-E and F-layer propagated ground scatter signals were read from the film and recorded on graphs. These graphs also recorded the azimuth of the various returns and their respective delays.

3. DATA REDUCTION

For the purpose of this report, the information present in the graphs referred to above was put into digital form. The

basic procedure was to record on punch cards the duration of the FAE and average delay, correct to the nearest millisecond for each hour of the day. The azimuth of these echoes, i.e., obtained from either the NW or NE quadrant, was also recorded. The quadrant behavior, however, is to be treated with caution due to the broad beamwidth (about 45°) of the antenna used. When FAE's were observed, it was noted from the graphs whether sporadic-E or F-layer supported groundscatter was simultaneously present in the same quadrant. Results were recorded on the cards. The 3-hour magnetic activity index K_{Fr} obtained from Fredericksburg, Virginia or Fort Belvoir, Virginia was also put on these cards. It is to be mentioned that Fredericksburg is a few degrees to the south of the station whereas the FAE's are obtained from the north. However, Fredericksburg is in the same longitude zone as the observing site and this is considered important in the separation of diurnal and magnetic activity dependence of FAE's. The hours in which there was equipment failure were excluded from the analysis.

The punch cards were first sorted by range to distinguish between FAE(E) and FAE(F). It was found - and range scatter plots will also show this - that echoes which were obtained with delays less than six milliseconds (msec) were E-layer echoes. Any echoes obtained at greater ranges are presumed to be either direct F-layer echoes or a combination of multi-hop propagation and field alignment. Each of these two broad categories are then subdivided according to the K_{Fr} index. A range of K_{Fr} from 0-3 is considered to represent average quiet conditions, whereas K_{Fr} ranging from 4-9 represents disturbed conditions. Later sorting on the basis of K_{Fr} alone will justify this grouping.

The data, after being divided into the four categories mentioned above, were sorted to yield the percentage occurrence in each hour for a particular month. This is an <u>actual</u> percentage of occurrence obtained by dividing the number of hours the FAE was present in that particular hour of the month by the total

number of samples available for the same month. Other groups, such as that working at Washington State University (Keck and Hower, 1968) have used a definition whereby an occurrence of FAE for more than 5 minutes in an hour is considered to be an occurrence for the whole of that hour. Thus it is difficult to compare occurrence statistics among various groups of workers.

4. DATA PRESENTATION

The behavior of the FAE's observed at Plum Island throughout the years 1961-65 is presented in the form of a series of histograms showing the diurnal variation of their percentage occurrence. We shall discuss the characteristics of each type of echo separately.

4.1 Occurrence of FAE(E)

The occurrence of FAE(E) for the five years of observation is shown in Figures 2 through 7. Each diagram represents 12 months of data. The first half of each hour represents percentage occurrence of echoes obtained from the NW quadrant in that entire hour, whereas the second half represents the echoes from the NE quadrant for that same hour. The shading within the occurrence blocks shows the fraction of time for which sporadic-E supported groundscatter was simultaneously present. Figures 2 through 6 represent individual months for quiet conditions, whereas Figure 7 represents average disturbed months over the five years of observation, the samples being statistically insignificant for each month separately. The number of samples in Figures 2 through 6 range from a low of 18 (when there were many disturbed periods) to a maximum of 31. The month of December 1965 has about half as much data as the other months because the observations were terminated in the middle of the month. Equipment failure occurred very rarely. Figure 7,

even though an average over 5 years, has a similar number of samples in each block except for a few daytime blocks when there are less than ten samples.

The first obvious pattern of the quiet day FAE(E) is its occurrence in the evening, nighttime, and early morning hours. There is virtually no daytime FAE(E). There is a greater incidence during the solstices than during the equinoxes, with the summer maximum being higher than that in the winter. The winter months, having a longer period of darkness, show echo activity more uniformly distributed over a longer period of time than do the summer months. The increased occurrence during the solstice period is usually accompanied by increased sporadic-E supported propagation occurring simultaneously. This leads us to believe that there is a high degree of field-alignment in the sporadic-E patches that appear to the north of the station during the evening hours of the summer and winter months. The equinoctial periods are characterized by little or no occurrence at all, and very little of the FAE(E) that is present is accompanied by the sporadic-E type propagation so common in the summer. Thus there is a distinct seasonal dependence as well as diurnal dependence of quiet time FAE(E). One other obvious feature in these diagrams is the greater incidence of echo activity from the NW as compared to the NE. This asymmetry becomes self-explanatory when the geometry of the station as shown in Figure 1 is taken into consideration. Since the magnetic pole is to the NW of the station, a much greater degree of field alignment is possible in that direction.

Figure 7, representing the average monthly behavior of FAE(E)'s over the five years of observation during magnetically disturbed conditions (K_{Fr} 4-9), shows many features which are different from the quiet time behavior. A uniformly higher nighttime percentage occurrence is obtained throughout the year, thus obliterating any seasonal differences. In addition, much more daytime activity is evident in the afternoon hours. The

summer and winter months, even though they have greater echo activity, have much less supporting sporadic-E propagation. This suggests that periods of magnetic activity tend to inhibit the formation of sporadic E. A similar E-W asymmetry is somewhat reduced, leading us to believe that during periods of greater magnetic activity the irregularities have a greater density and are received by a broad beam angle antenna at all northern azimuths.

4.2 Occurrence of FAE(F)

The characteristics of the field aligned F-layer echoes are discussed in this section. This is a more complex phenomenon than the E-layer backscatter where orthogonality considerations are universally met. The monthly percentage occurrence curves are presented in Figures 8 through 13 following the same general procedure as for the FAE(E). The only difference is that the shading in this case represents the fraction of time for which the FAE(F) were accompanied by F-layer propagated groundscatter. This gives us an idea of the amount of refraction available to produce orthogonality at F-layer heights. The most obvious feature of the quiet day histograms (Figures 8-12) is the sunset peak of occurrence of these echoes. The peak is present throughout the year, but the equinoxes show more activity than the solstices. It must be remembered that there is a great deal of FAE(E) during the solstices which reduces the energy reaching F-layer heights.

A closer look at the diagrams shows that the peak echo activity shifts with the time of sunset - the peak occurs earlier in winter and much later in summer, a fact already pointed out by Malik and Aarons (1964). The supporting groundscatter pattern follows the echo pattern, and it is the gradual decrease of the groundscatter later in the evening that is responsible for the tapering off seen in the echo activity. This will be more clearly seen in the groundscatter contour

diagrams to be presented in a later report. From scintillation boundary concepts (Aarons and Allen, 1971), we know that the late evening and midnight hours are precisely those during which we expect an increased probability of finding F-layer field aligned irregularities at the latitudes of interest. However, the decay in underlying ionization at these hours makes it impossible for the ray to achieve orthogonality at the higher heights.

Some daytime backscatter is evident, almost all of it entirely supported by groundscatter. This shows that during the daytime refraction is adequate, but the absence of irregularities is the usual limiting factor. It is interesting to note that there is hardly any daytime backscatter activity during the summer which is probably due to the high incidence of E_s. We shall see later that most of the daytime FAE(F) observed have large delay times. There is a great deal of year-to-year variability in the occurrence statistics - in general the higher sunspot years showing greater activity.

The average behavior of the disturbed day FAE(F) is shown in Figure 13. As in Figure 7, each month represents the mean over five years of observation. There is an increase in the daytime backscatter throughout the year except during the summer months. There is also a shift in the sunset peak towards earlier hours of the afternoon. We shall further discuss the disturbed day features later in the report.

5. RANGE DISTRIBUTION OF FAE.

The range distribution of FAE's is presented in Figures 14 and 16 through 18 on an individual seasonal basis to determine, if possible, the most probable ranges for FAE(E) and FAE(F). The diagrams include backscatter from both quiet and disturbed days in each season. The seasons are defined such that spring

represents Feb-Apr; summer, May-July; fall, Aug-Oct; and winter, Nov-Jan. The ordinate represents the total number of hours of backscatter echo obtained with delays ranging between 2 and 25 msec. It is to be emphasized that these are not percentage occurrence curves, but each seasonal curve shows the total number of hours of echo obtained in a particular season out of a possible maximum of roughly 90 x 24 = 2160 hours. The graphs are not shown as histograms in order to facilitate the superposition of data obtained during the five consecutive years.

Each seasonal curve clearly shows a maximum around 3-4 msec delay and again around 7-9 msec delay with a distinct minimum at 5 msec. Thus it is quite reasonable to assume that the echoes represented by delays less than 6 msec are FAE(E), whereas the echoes obtained at delays $\geq$ 6 msec originate in the F layer. The range corresponding to each millisecond is 150 km for free space propagation. Referring to Figure 1a, we find that for an E-layer height of 110 km, delays of 3-4 msec correspond to elevation angles of 6°-10°, and for azimuths centered around magnetic north, these delays correspond to propagation angles ranging between 89°-91°. A direct comparison with Figure 1b is unjustified for the E-layer echoes, as considerable refraction makes the ray paths deviate greatly from idealized straight line paths on which this diagram is based. In addition, there is a much greater variability in the height of the F layer.

The long range field aligned echoes, though only a small fraction of the regular FAE(F), show certain interesting features. All the seasons show small peaks around 13-14 msec, another close to 18-19 msec, and a very small one near 22-23 msec. The first two of these roughly correspond to a 2F1E mode and a 3F2E mode respectively, in terms of their observed delay as shown in Figure 15. It should be noted that for the 2F1E mode the field alignment is in the E layer, whereas for the 3F2E mode the field alignment is in the F layer. Later diagrams will show that these long range echoes are observed

only in the daytime when there is sufficient ionization in the E layer and the F layer. The possibility of observing such modes of propagation has been demonstrated by Agy (1971) using ray tracings through a model high-latitude ionosphere. The radar used being of low power, these modes have the added advantage of a minimum number of traversals through the absorbing D region.

Figures 16 through 18 show similar characteristics for the three other seasons. Figure 16 which represents summer conditions is somewhat different in as much as no long-range echoes are observed. The decrease in F-layer activity may be attributed to two causes: (1) the summer decrease in f_0F2 which decreases refraction and (2) the high incidence of sporadic E which severely decreases the energy reaching F-layer heights. Figure 18 representing winter conditions has only four graphs superposed on it since winter 1965 was not complete, observations having been stopped in the middle of December. The interesting point to note on this graph is the relatively large peak at 22 msec which is probably due to the ground supported 3F mode with field alignment in the F layer as shown in Figure 15. The winter f_0F2 being the highest and f_0E being the lowest of any season in the year, conditions for observing such a mode should be most favorable in the winter.

To show the diurnal variation of the range of echoes in any given year, the day was divided into 3 different time periods: a daytime period between 0600 and 1800 hours, a sunset and pre-midnight period between 1800 and 2400 hours, and finally the post-midnight period between 0000 and 0600 hours. The resulting graphs for the years 1961 and 1964 are shown in Figures 19 and 20. All the long-range echoes are confined to the daytime period, the evening hours show both E-layer and F-layer activity, whereas the post-midnight period shows only E-layer activity. It is interesting to note that the horizon for an altitude of 300 km is represented by a distance of approximately 2000 km which corresponds to a delay of 13 msec.

As such, all the activity in the evening hours can be explained in terms of direct reflections from the E and F layers, and those in the post-midnight period from the E layer alone. The daytime long-range echoes are, however, obtained from distances far beyond the northern horizon where the probability of encountering daytime irregularities is much enhanced. The year 1964 (Figure 20) shows reduced long range echo activity because of the reduced solar activity being indicated by the very low sunspot numbers (Figure 28). The percentage of all echoes obtained with a particular delay are shown in Figure 21 for the years 1961 and 1964. The other years, with sunspot numbers intermediate to those of these two years, have comparable behavior. In order to get an idea of the total occurrence of backscatter, it should be mentioned that backscatter occurred for only 6% of the time throughout 1961, and of all the occurrence noted, only 5% was of the long range kind, i.e., with delays greater than 13 msec.

6. AVERAGE SEASONAL BEHAVIOR OF FAE

The average seasonal behavior of FAE(E) during both quiet and disturbed magnetic periods is shown in Figure 22. The quiet periods represent approximately 400 hours of data while the disturbed periods range from 25 to 100 hours with the majority of time-blocks ranging between 40-60 hours. As pointed out earlier, the increased occurrence of FAE(E) during magnetic storms is very prominent in all four seasons. In addition to the increased evening and nighttime occurrence, there is a great deal of daytime occurrence. In fact, virtually all the daytime occurrence during these five years is during disturbed periods. The other interesting feature is the decrease of simultaneous E_s-supported propagation that accompanies the increase of FAE(E)'s during storms. This suggests that magnetic storms

inhibit the formation of E_s clouds. However, an influx of charged particles at E-layer heights is responsible for the enhanced FAE(E) (Paulikas, 1971).

A similar diagram for FAE(F) is shown in Figure 23. Here, too, we find the same obvious increase with increased magnetic activity, except during the summer where the opposite seems to be true. The summer storms at these latitudes are usually followed by a large depletion of the F layer (Mendillo et al, 1969), and this reduced ionization seems to be responsible for the decreased FAE(F). There is some daytime occurrence of high backscatter even during quiet days. As a matter of fact, all the long-range backscatter ($\geq$ 13 msec) shown in Figures 14, 17, and 18 were obtained during quiet pericds. There is an increase of daytime backscatter during disturbed periods but they are all of the direct-F kind. It seems that during any magnetic storm situation there is some depletion of the bottom-side F layer as well as increased absorption which is adequate to block out the long-range echoes.

7. FAE AS A FUNCTION OF MAGNETIC ACTIVITY

We have seen that generally both FAE(E) and FAE(F) increase with magnetic activity. So far, however, we have considered two ranges of activity only. To study in detail the dependence of backscatter on the level of magnetic activity, the FAE data was sorted according to the K_{Fr} index. The result for the case of E-layer irregularities is shown in Figure 24a, in which the percentage occurrence of echoes is plotted as a function of K_{Fr}. The data represents the entire five year period under consideration, and the number of hours of observation belonging to each K interval are indicated on the diagram. As before, the first half of each K interval represents returns coming from the NW, and the second half from the NE. The sample size becomes

rather small for K indices ranging 7-9. It is very obvious from this graph that the E-layer backscatter is a very sensitive function of the K index. Between K indices of 0-3 there is the usual E-W asymmetry in the incidence of echoes, but the percentage occurrence remains small. Beyond $K_{Fr} \geq 4$, the percentage occurrence increases with each integral increase of K. It finally levels off for $K_{Fr} \geq 6$, and the degree of asymmetry levels off also, because irregularities appear at all northern azimuths during severe magnetic storms. Figures 24b and 24c show the same data when separated into daytime (0600-1800) and nighttime (1800-0600) hours. Figure 24b shows the total lack of FAE(E) during the daytime for K range 0-3, and a pronounced increase beyond that range. The nighttime hours show a gradual increase for the low indices with the same prominent increase for the high ones.

Similar diagrams for the F-layer backscatter are shown in Figures 25a-c. The total occurrence characteristics are greatly reduced - note the magnified occurrence scale. However it is interesting to note the monotonic increase of occurrence with K index up to a value of K=4, beyond which the occurrence tapers off becoming zero for $K \geq 7$. Now, from scintillation studies (Aarons et al, 1963), it is a well known fact that the incidence of irregularities increases with K_{Fr}. Thus the decrease in the FAE(F) is to be attributed to the depletion in the underlying ionization during severe magnetic storms. The daytime situation alone (Figure 25b) represents the 24 hour picture, as the nighttime occurrence (Figure 25c) is insignificant. We have seen earlier (Figures 19 and 20) that all of this low nighttime occurrence takes place in the pre-midnight hours. The shading within the histograms, which represents supporting F-layer propagated groundscatter echoes, shows a behavior similar to that of the field aligned echoes, i.e., increasing in proportion to the increased echo occurrence and then tapering off during severe storms.

8. SOLAR CYCLE DEPENDENCE OF FAE

To study the solar cycle dependence of the field aligned echoes, if any, percentage occurrence contours of both E-layer and F-layer echoes were drawn for the entire five year period of observation. The data base was restricted to quiet magnetic conditions, and the occurrence statistics in the NW quadrant were used for drawing the contours.

The FAE(E) contours are shown in Figure 26. The yearly summer maximum during the evening and nighttime hours is the most distinctive feature. There is a much weaker but quite definite secondary winter maximum. No definite solar cycle dependence is discernible from the contours. A reference to Figures 19 and 20 shows that there were more hours of FAE(E) in 1961 than in 1964. However, it is difficult to come to a definite conclusion with the limited solar cycle coverage available.

The FAE(F) contours (Figure 27), show a positive dependence on the solar cycle. There is a gradual decrease in the incidence of echoes from 1961 to 1964, and then an upward trend is observed in 1965. The rough sinusoidal pattern of echo occurrence is evident as it follows the time of sunset throughout the seasons, the echo onset being much earlier in winter than in summer. The mean monthly Zurich sunspot numbers for the period 1961-65 are shown in Figure 28. Though a general trend is clearly visible, there is much month-to-month variability indicating that this kind of variability should be expected in the FAE data also.

9. SUMMARY AND CONCLUSIONS

This detailed study of field aligned irregularities in the E and F layers of the ionosphere has yielded valuable information regarding the diurnal, seasonal, and geomagnetic control of the occurrence statistics. The important characteristics of each

type of echo will be summarized below.

9.1 FAE(E)

1. FAE(E) mostly occur at delays of 3-4 msec and are more numerous in the NW quadrant which contains the magnetic pole.
2. During quiet magnetic conditions (K_{Fr} 0-3), FAE(E) are confined to the late evening and nighttime hours.
3. FAE(E) shows a very definite maximum during the summer months. A weaker maximum is observed in the winter. However, the diurnal variation mentioned in (2) is always observed irrespective of season. The summer FAE(E) is mostly accompanied by simultaneous ground-scattered E_s echoes.
4. Geomagnetic activity increases the occurrence of FAE(E). A great deal of daytime activity as well as increased nighttime activity is seen. No seasonal control is evident. A marked decrease of simultaneous ground-scattered E_s echoes is observed.
5. There is no clearly defined solar-cycle dependence of FAE(E) observed in the data.

9.2 FAE(F)

1. This type of echo is obtained only when sufficient underlying ionization makes it possible for the ray to achieve orthogonality with the geomagnetic field at F-layer heights. FAE(F) are mostly observed at delays of 7-9 msec and, like the FAE(E), occur mostly in the NW.
2. During quiet magnetic conditions FAE(F) are confined primarily to the sunset hours. Some daytime activity is observed with delay times ranging between 15-25 msec. These long-range echoes can be explained in terms of multi-hop propagation and field alignment.

3. The equinoxes show more activity than the solstices - this can be explained in part by the greater FAE(E) activity seen during the summer and winter, which decreases the amount of energy reaching the F layer. The time of the sunset peak naturally varies from season to season. The FAE(F) is generally accompanied by F-layer supported groundscatter echoes.
4. The dependence of FAE(F) on geomagnetic activity is very interesting. A monotonic increase of the daytime FAE(F) with K_{Fr} is observed until a threshold value is reached ($K_{Fr}=4$), beyond which the depletion of F-layer background ionization causes it to decrease. Complete cut-off is attained under severely disturbed conditions ($K_{Fr}\geq 7$).
5. The incidence of FAE(F) shows a positive correlation with the solar cycle.

10. FUTURE WORK

In the next report the occurrence characteristics of E_s-layer and F-layer supported groundscattered echoes will be presented. In addition, fE_s and f_oF2 of relevent ionospheric stations will be studied in an effort to explain the observed characteristics of field aligned echoes as well as ground-scattered echoes. It is hoped that the FAE(E) can be explained in terms of both the occurrence statistics of E_s and the equatorward movement of the auroral oval in times of magnetic disturbances. On the other hand, the diurnal pattern of the scintillation boundary under quiet and disturbed conditions, and the change in F-layer ionization as a function of time, latitude, season, and magnetic conditions, will be used to explain qualitatively the observed incidence of FAE(F).

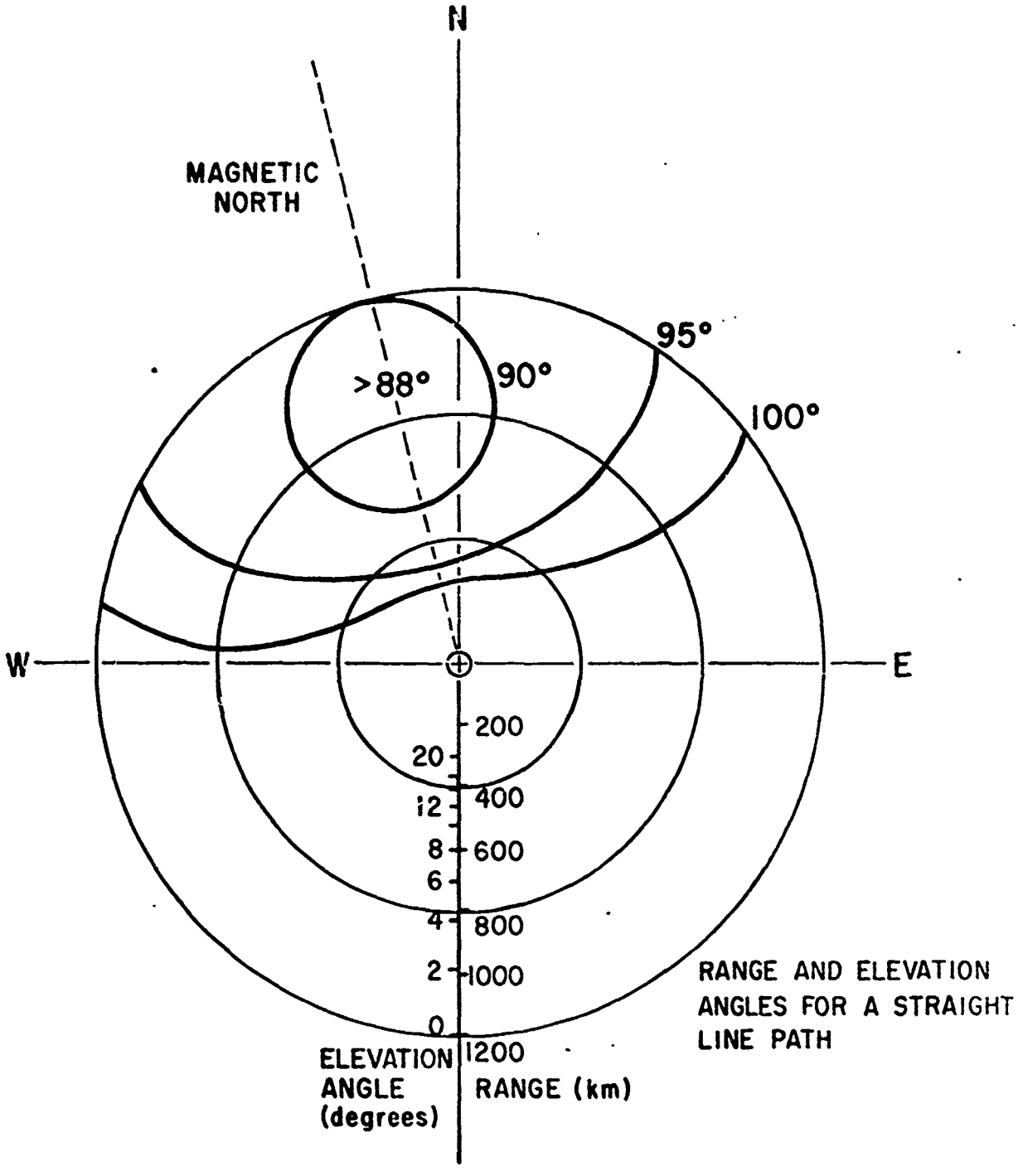

FIG. 1a PROPAGATION ANGLE CONTOURS FOR PLUM ISLAND MA AT 110 km HEIGHT.

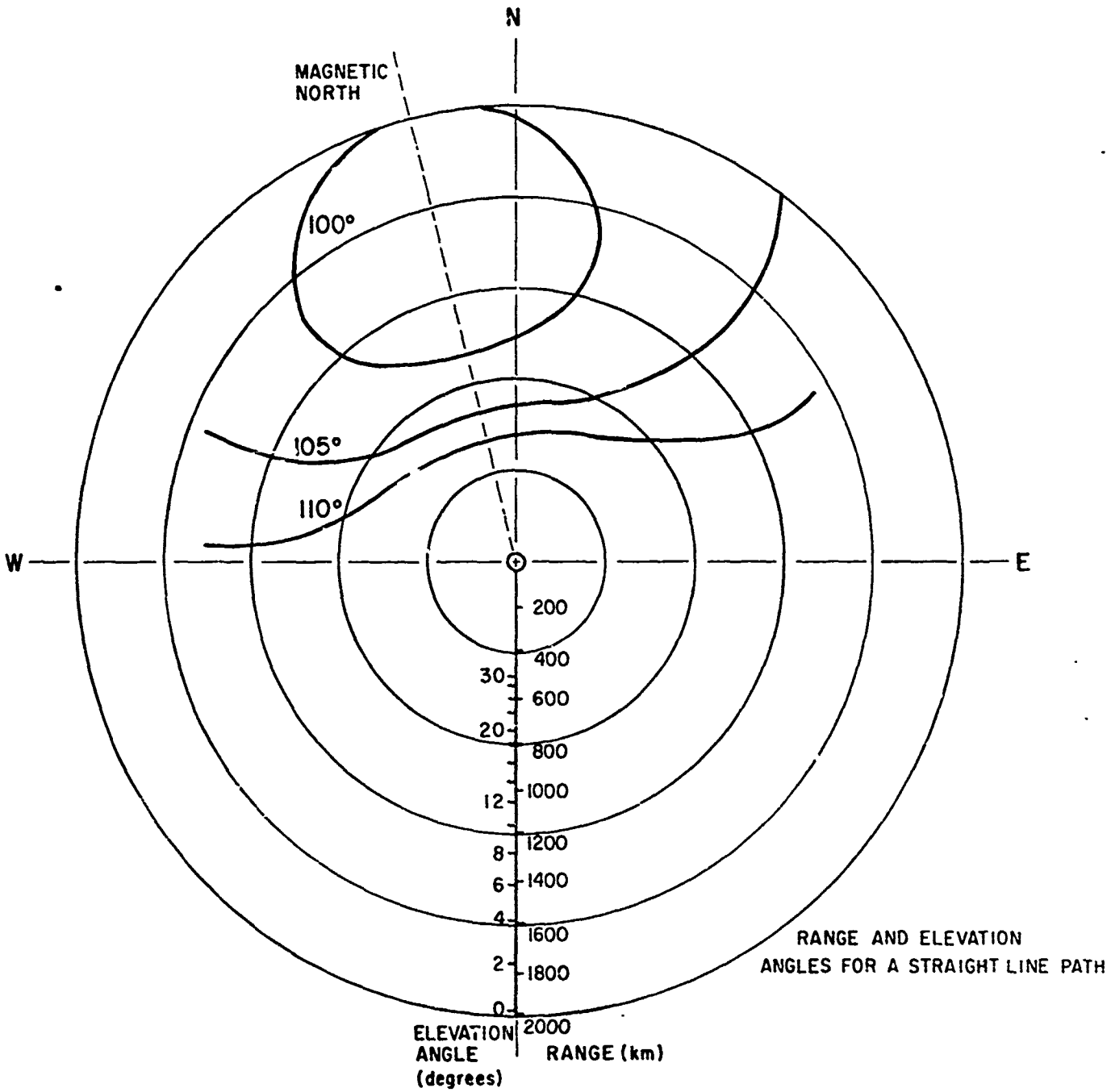

FIG. Ib PROPAGATION ANGLE CONTOURS FOR PLUM ISLAND MA AT 300 km HEIGHT.

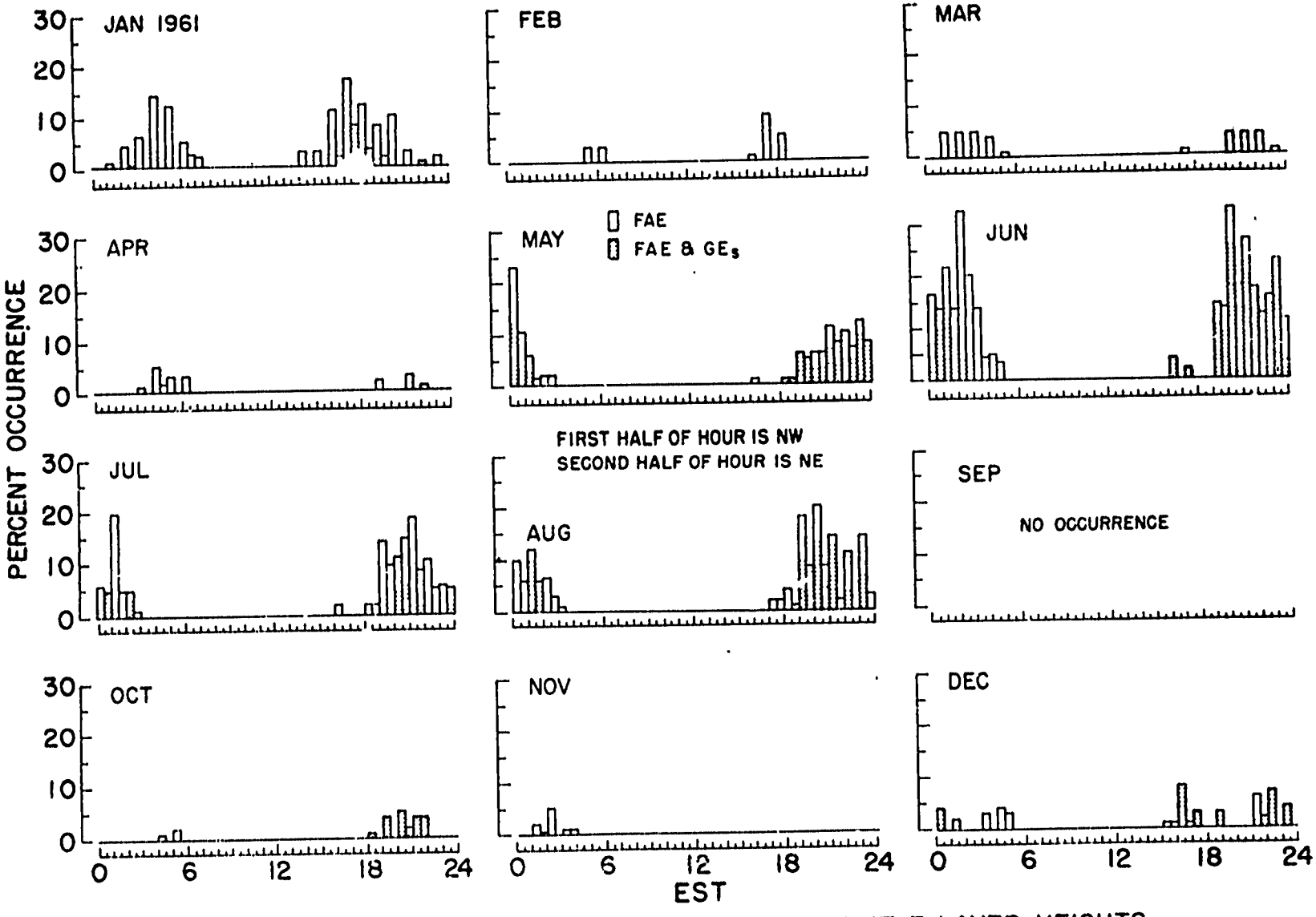

FIG. 2 BACKSCATTER FROM FIELD ALIGNED IRREGULARITIES AT E-LAYER HEIGHTS FOR K_{Fr} 0-3 DURING 1961

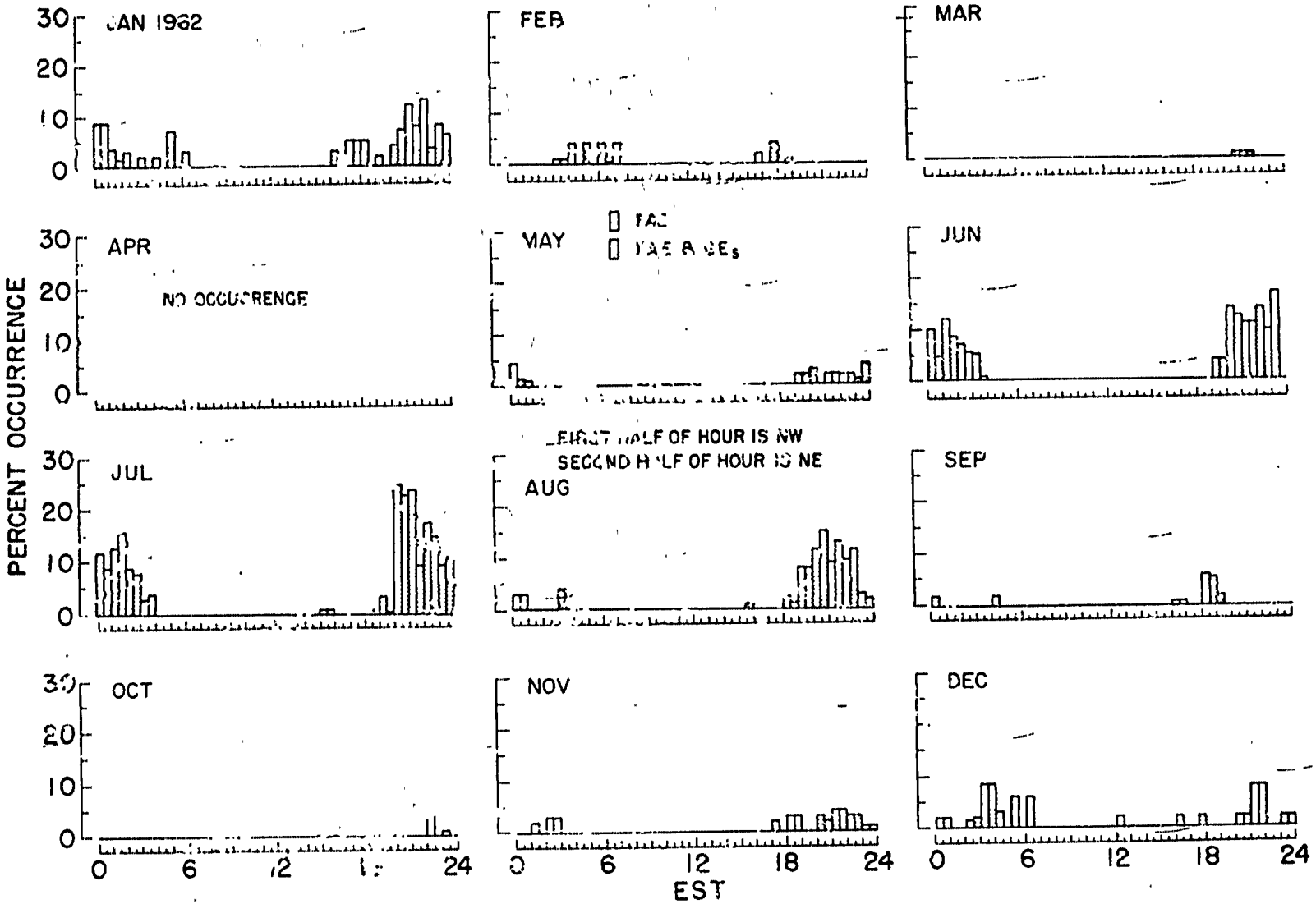

FIG. 3 BACKSCATTER FROM FIELD ALIGNED IRREGULARITIES AT E-LAYER HEIGHTS FOR K_p 0-3 DURING 1962

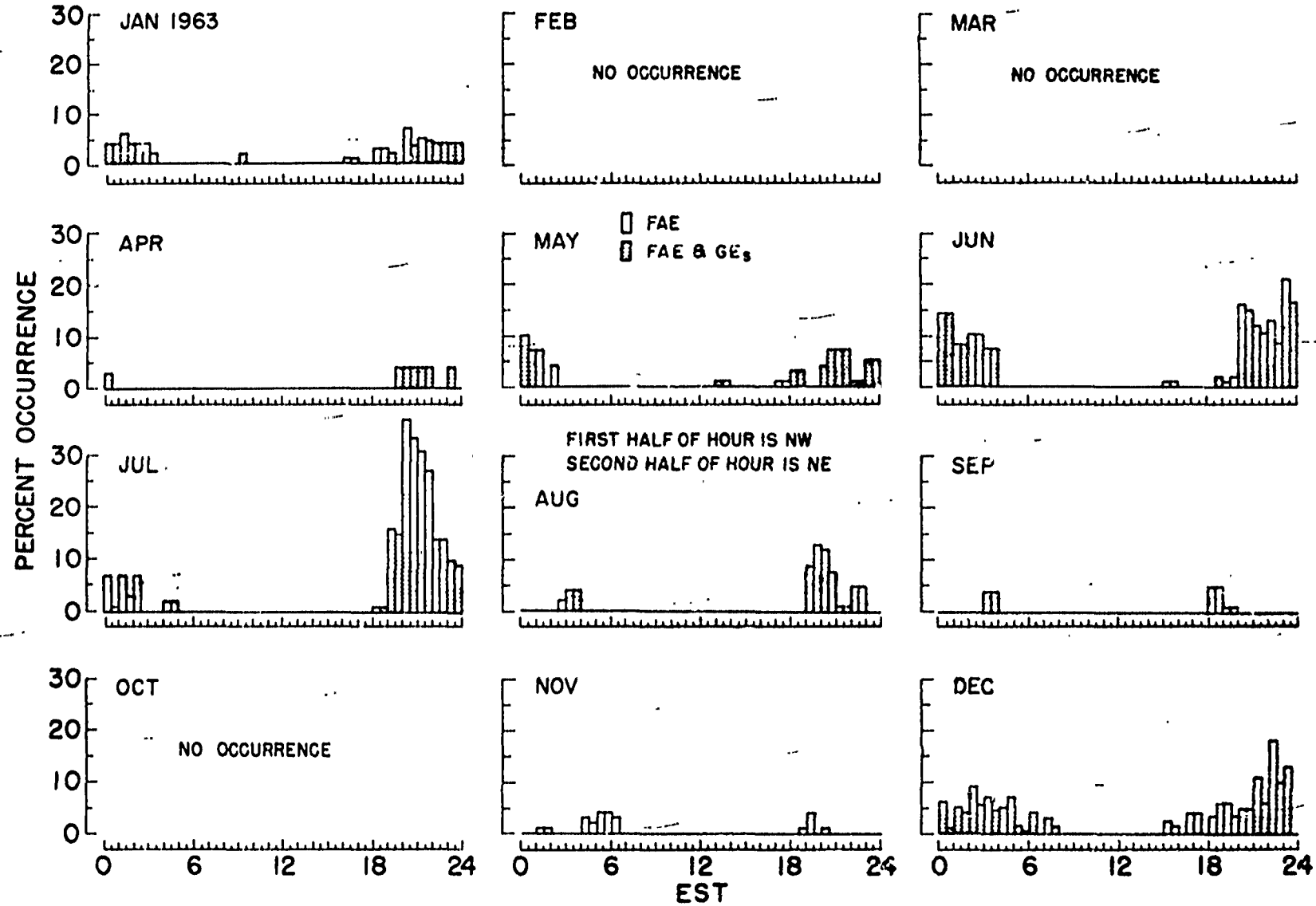

FIG. 4 BACKSCATTER FROM FIELD ALIGNED IRREGULARITIES AT E-LAYER HEIGHTS FOR K_{Fr} 0-3 DURING 1963

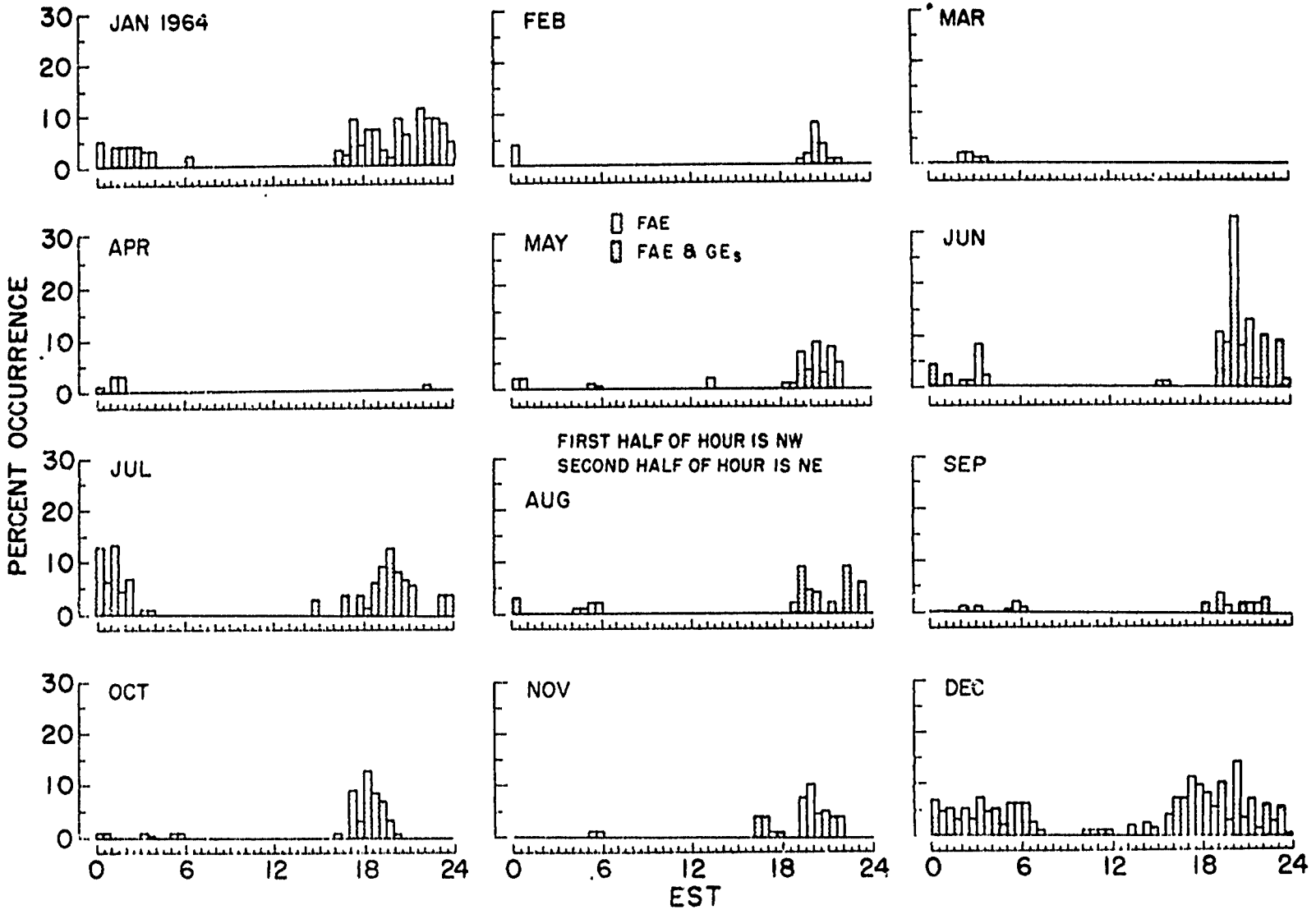

FIG. 5 BACKSCATTER FROM FIELD ALIGNED IRREGULARITIES AT E-LAYER HEIGHTS FOR K_{Fr} 0-3 DURING 1964

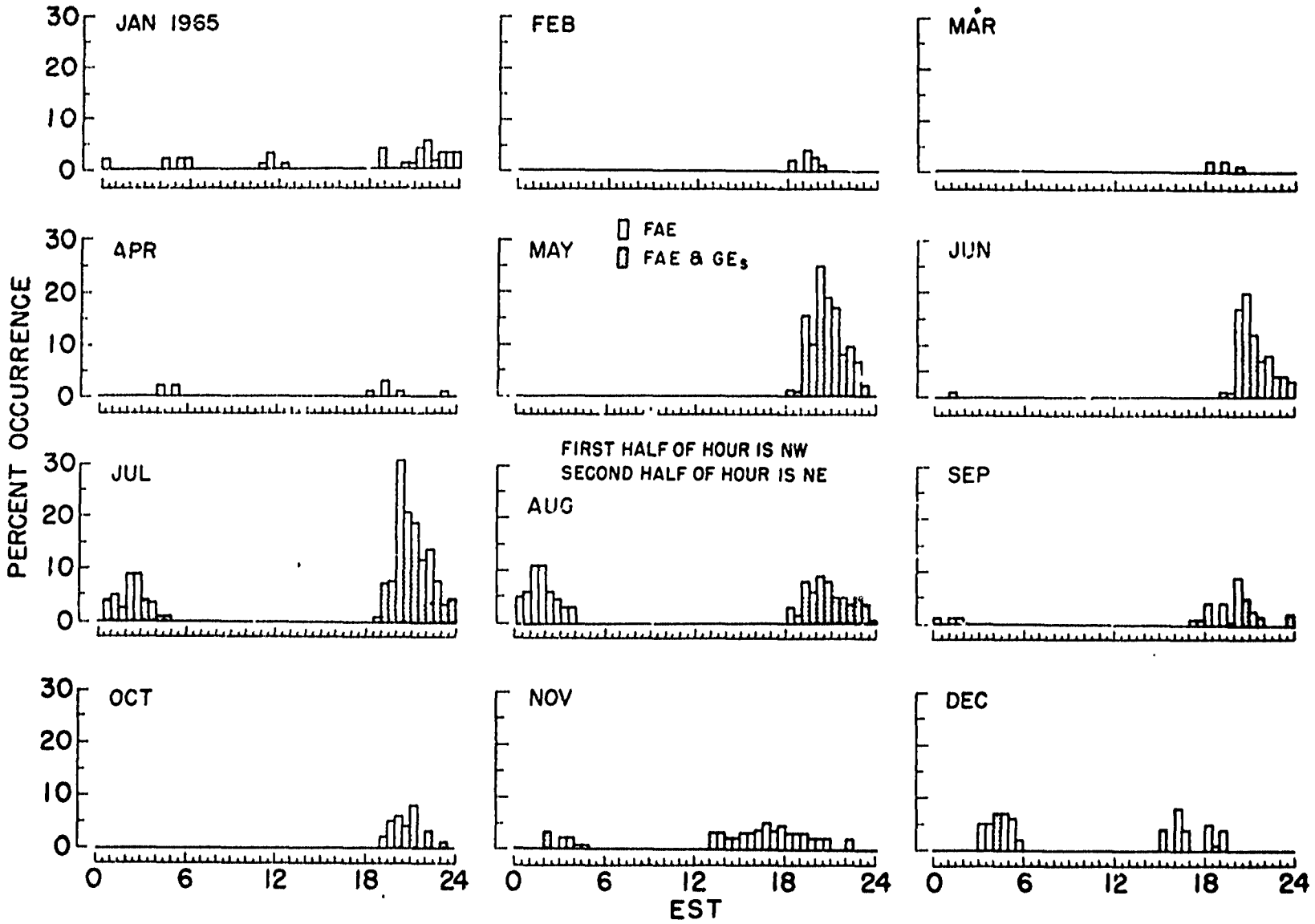

FIG. 6 BACKSCATTER FROM FIELD ALIGNED IRREGULARITIES AT E-LAYER HEIGHTS FOR K_{Fr} 0-3 DURING 1965

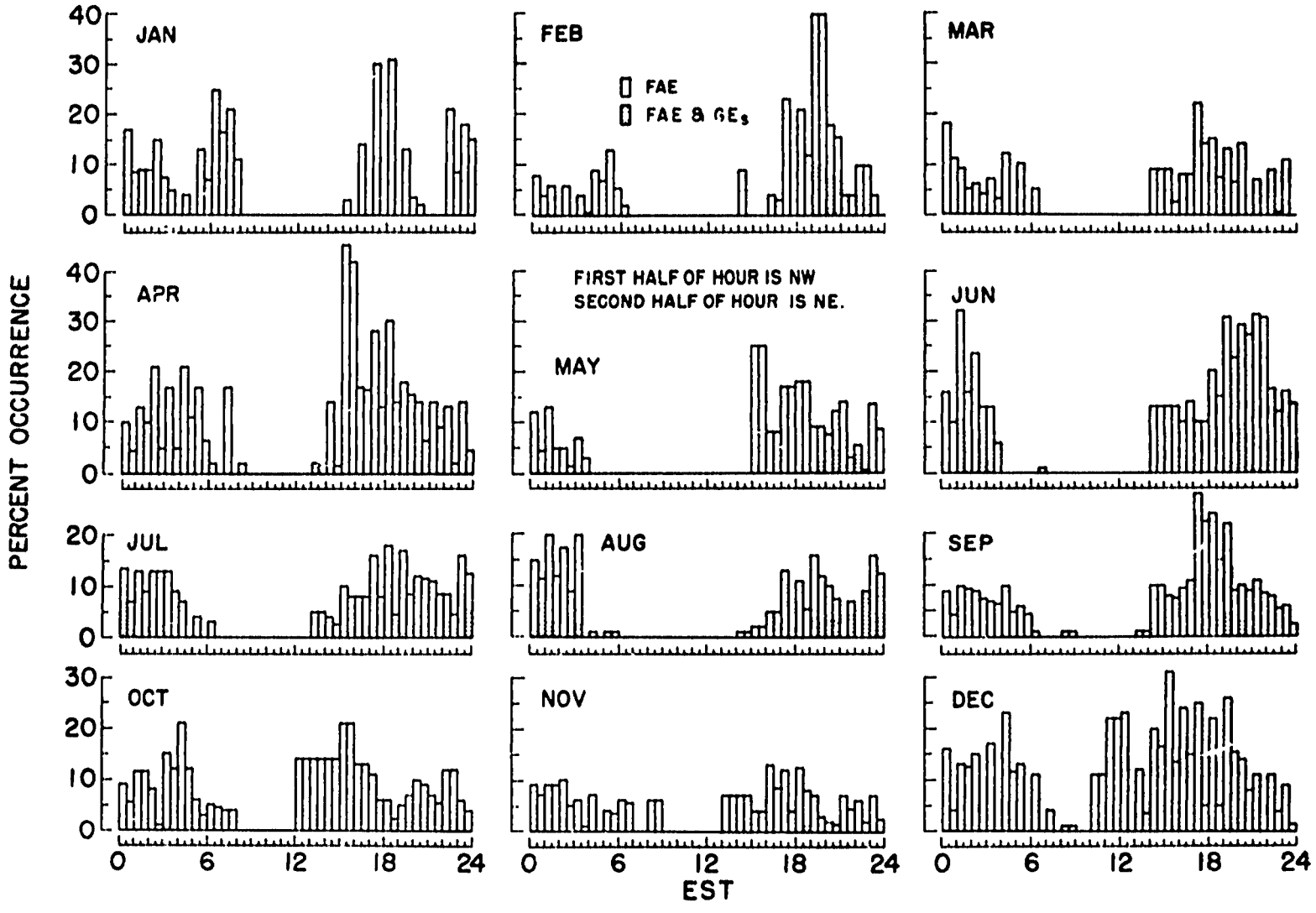

FIG. 7 AVERAGE E-LAYER BACKSCATTER FOR EACH MONTH FOR K_{Fr} 4-9 DURING 1961 - 1965

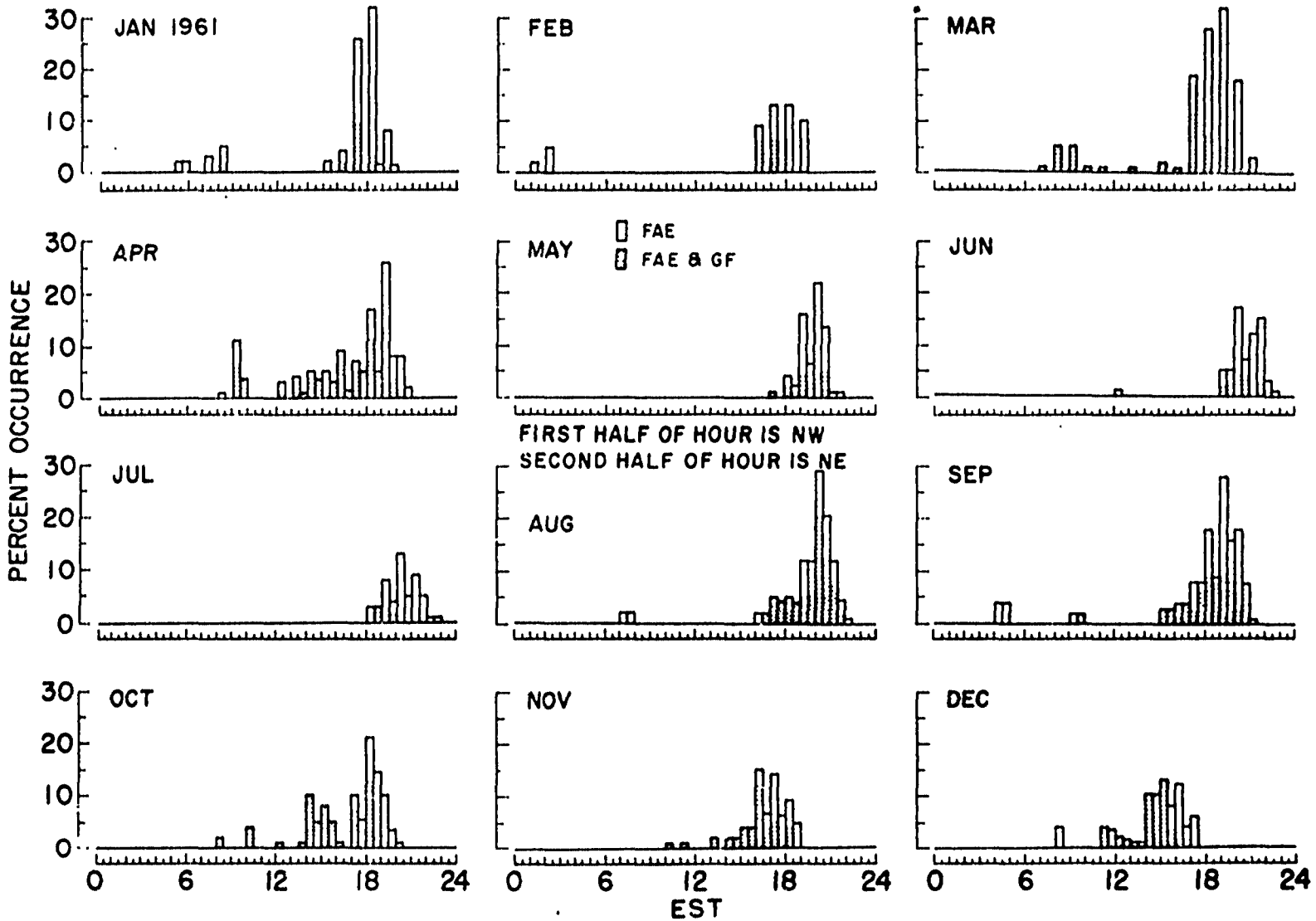

FIG. 8 BACKSCATTER FROM FIELD ALIGNED IRREGULARITIES AT F-LAYER HEIGHTS FOR K_{Fr} 0-3 DURING 1961

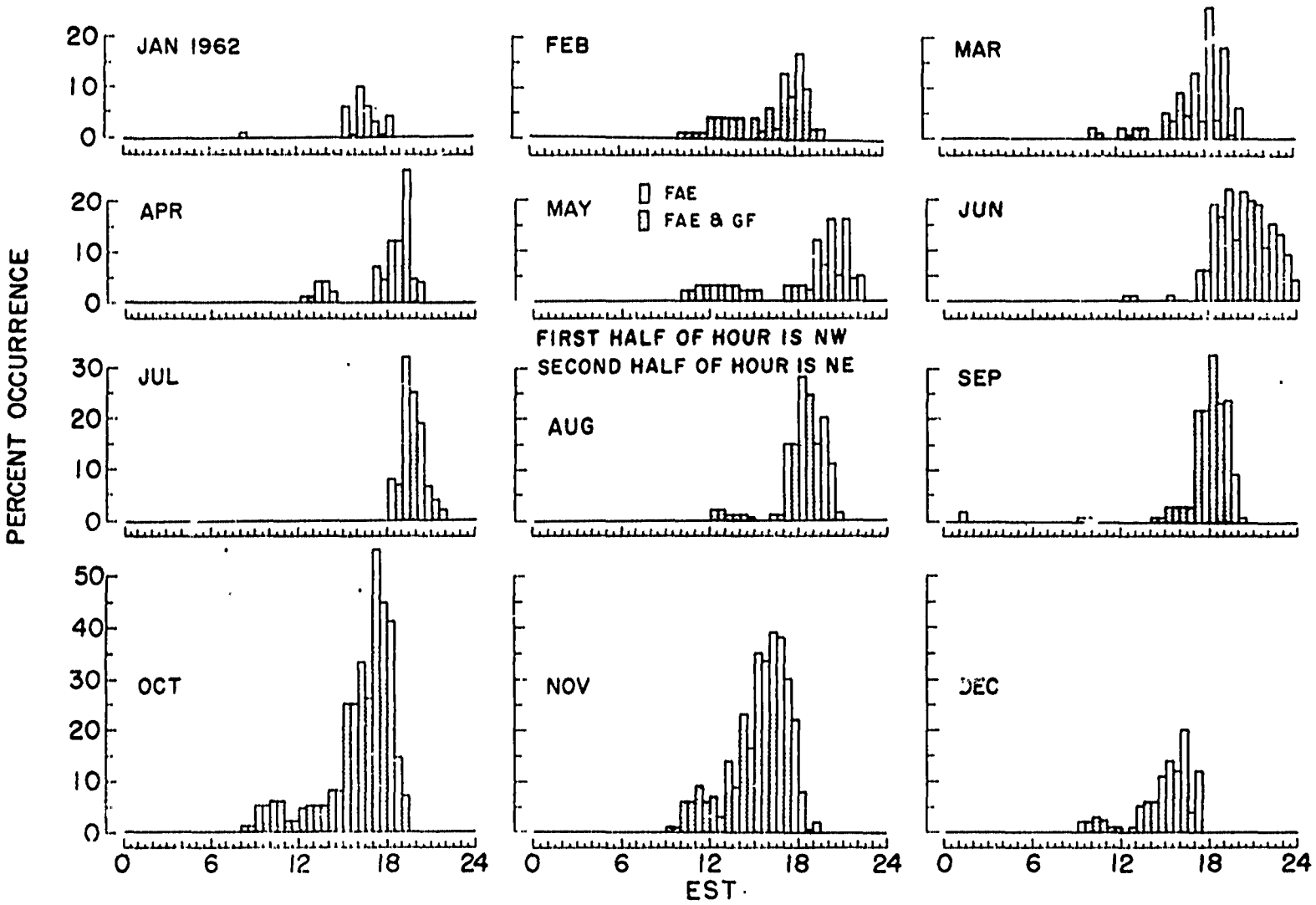

FIG. 9 BACKSCATTER FROM FIELD ALIGNED IRREGULARITIES AT F-LAYER HEIGHTS FOR K_{Fr} 0-3 DURING 1962

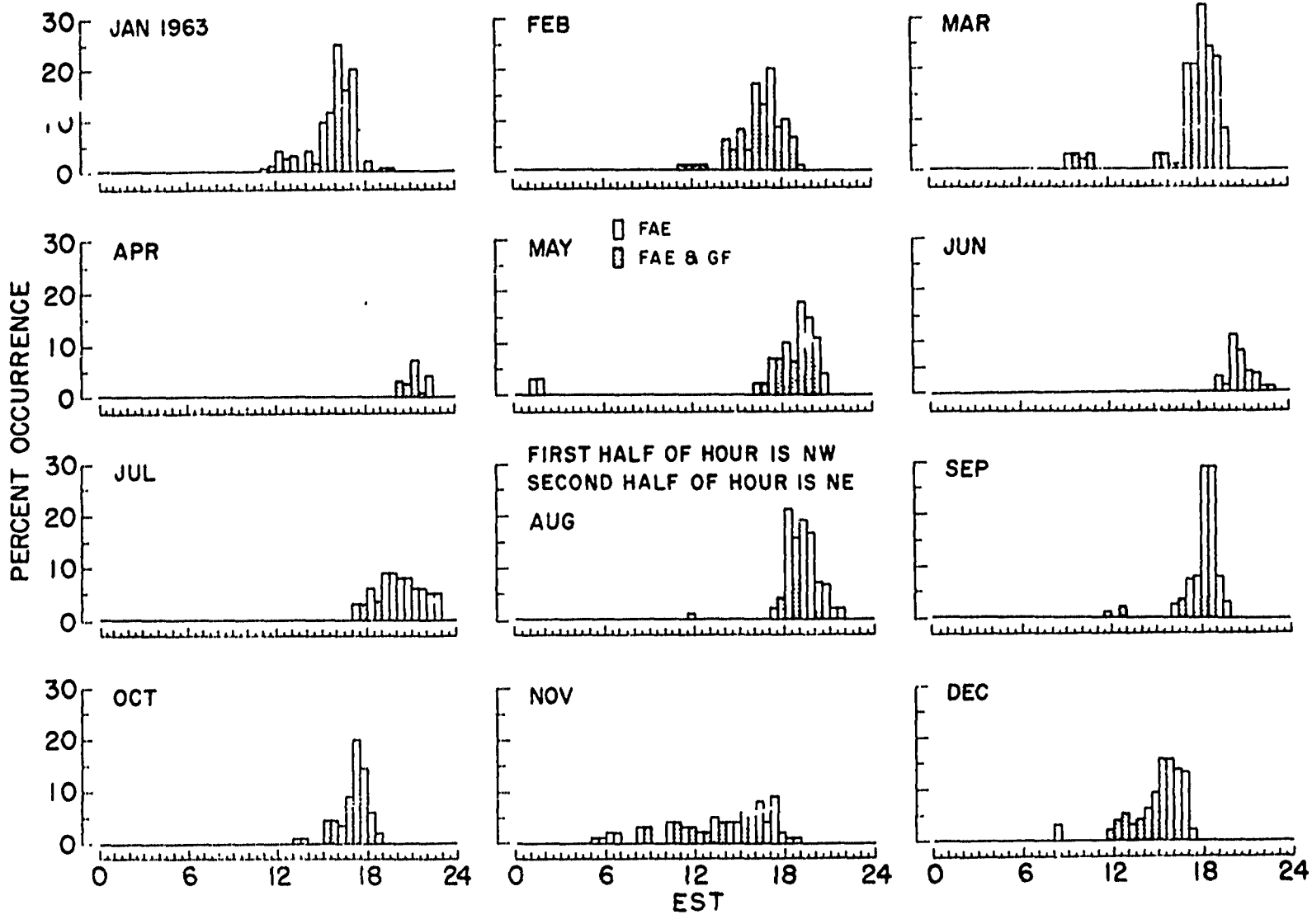

FIG. 10 BACKSCATTER FROM FIELD ALIGNED IRREGULARITIES AT F-LAYER HEIGHTS FOR K_{Fr} 0-3 DURING 1963

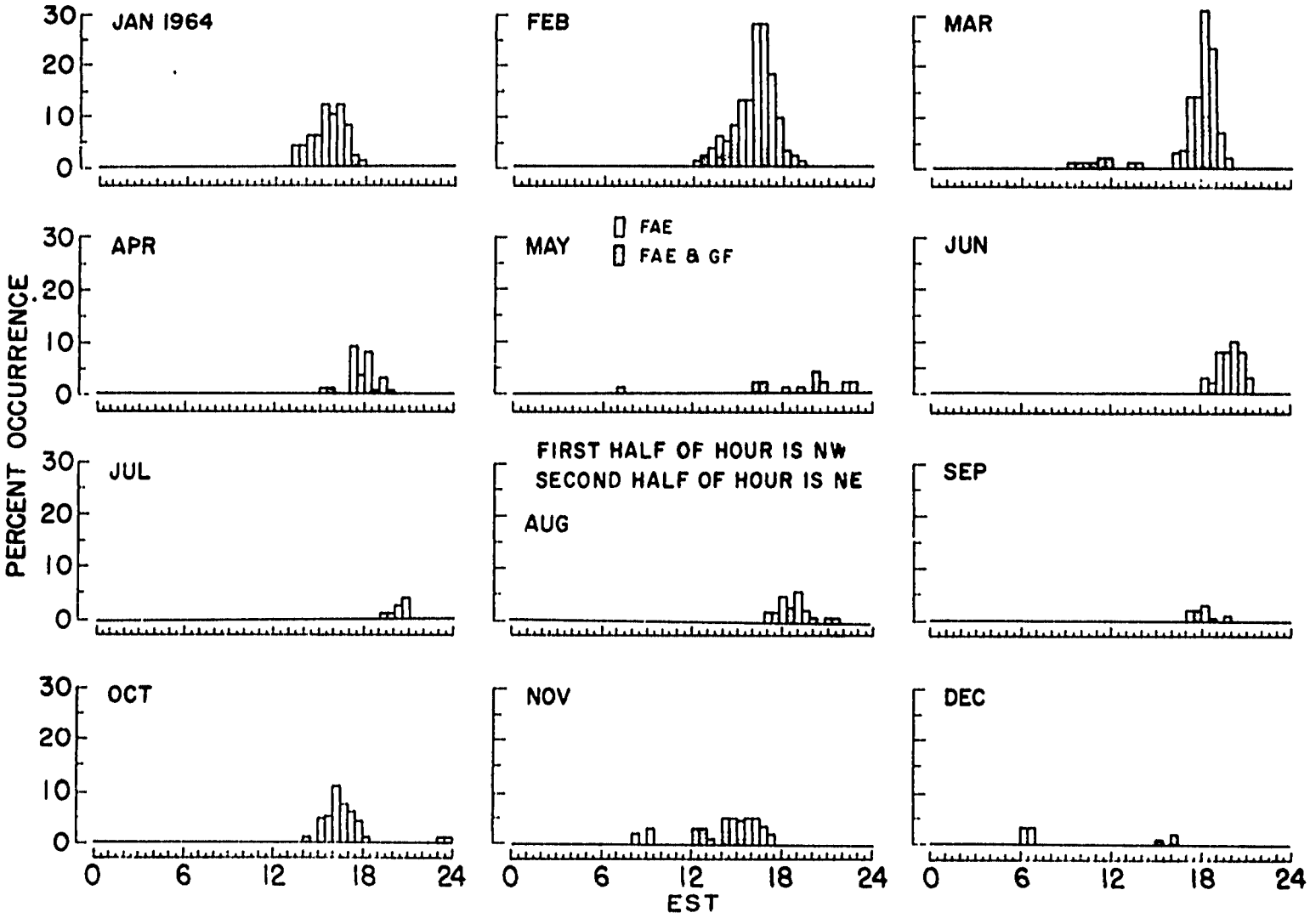

FIG. 11 BACKSCATTER FROM FIELD ALIGNED IRREGULARITIES AT F-LAYER HEIGHTS FOR K_{Fr} 0-3 DURING 1964

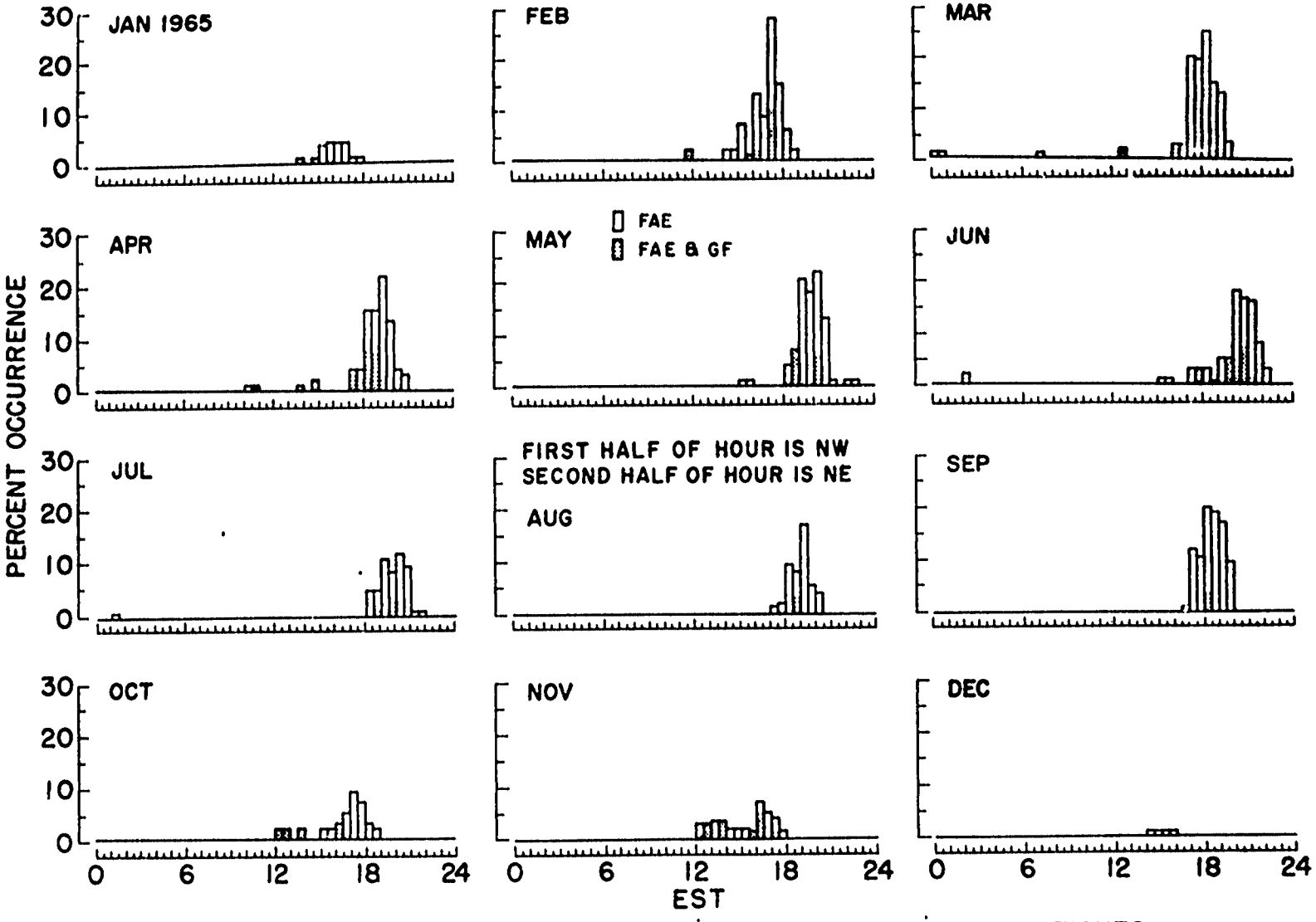

FIG. 12 BACKSCATTER FROM FIELD ALIGNED IRREGULARITIES AT F-LAYER HEIGHTS FOR K_{Fr} 0-3 DURING 1965

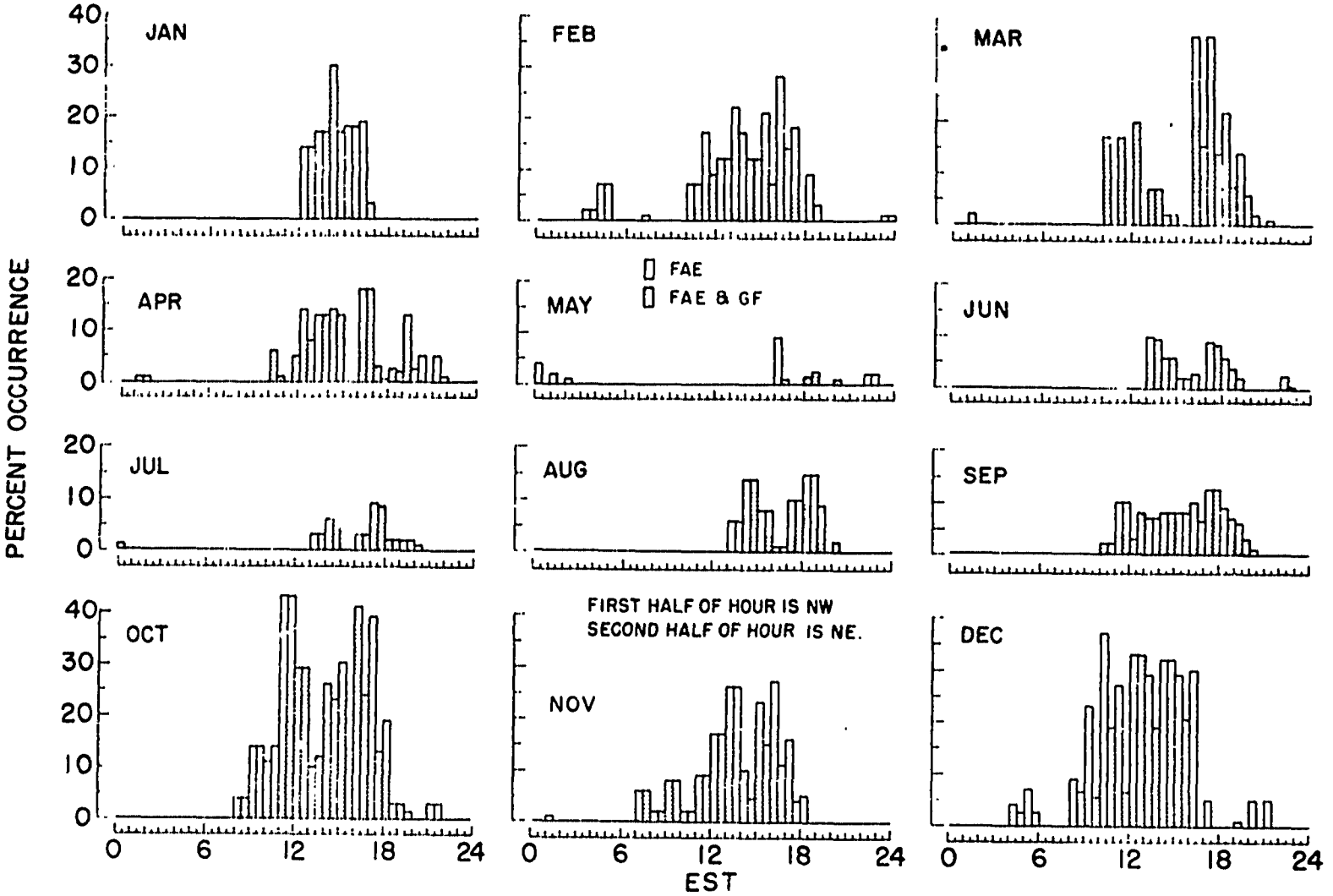

FIG. 13 AVERAGE F-LAYER BACKSCATTER FOR EACH MONTH FOR K_{Fr} 4-9 DURING 1961 - 1965

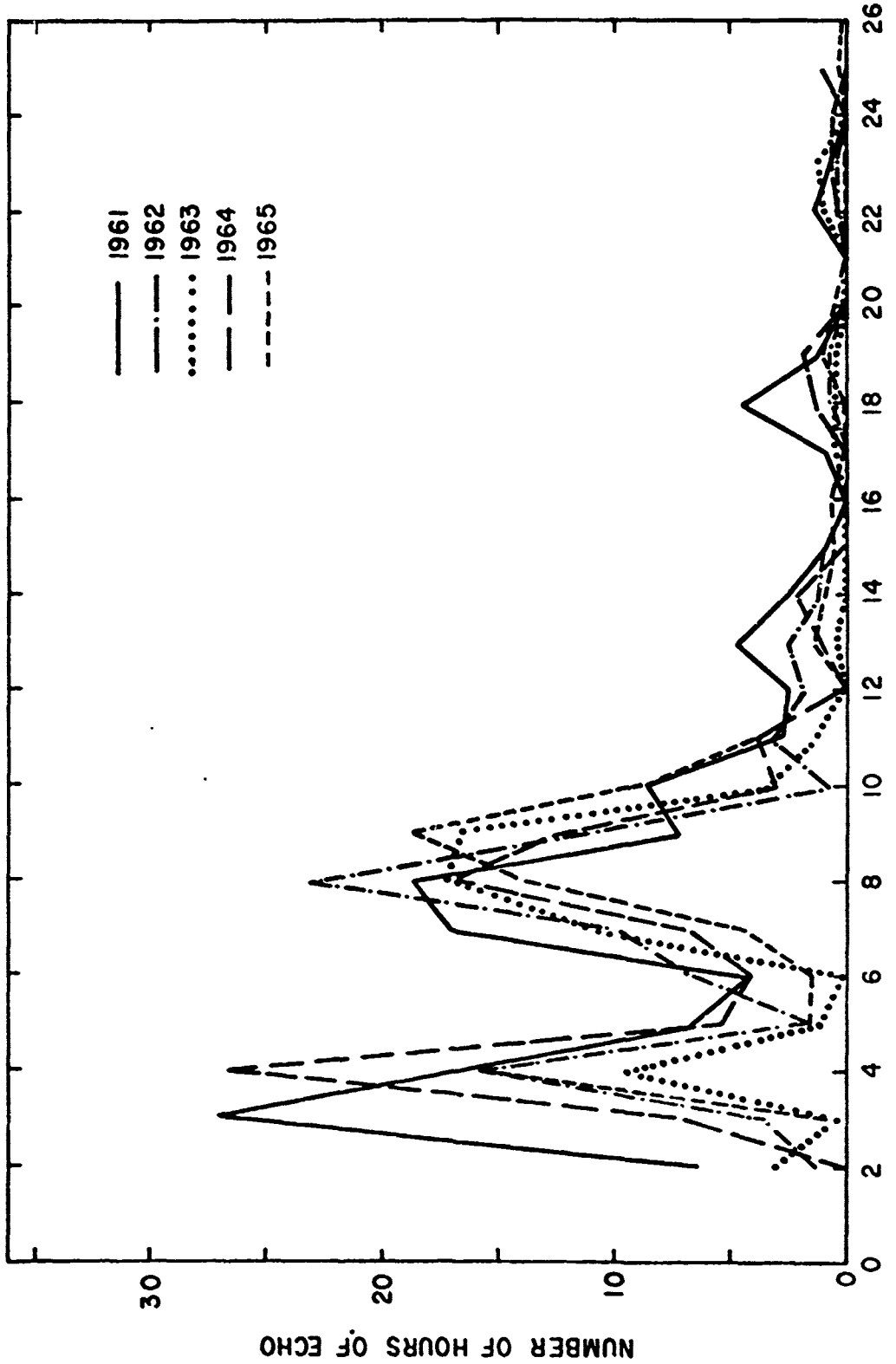

FIG. 14. RANGE DISTRIBUTION OF FAE's DURING THE SPRING SEASON, 1961-1965

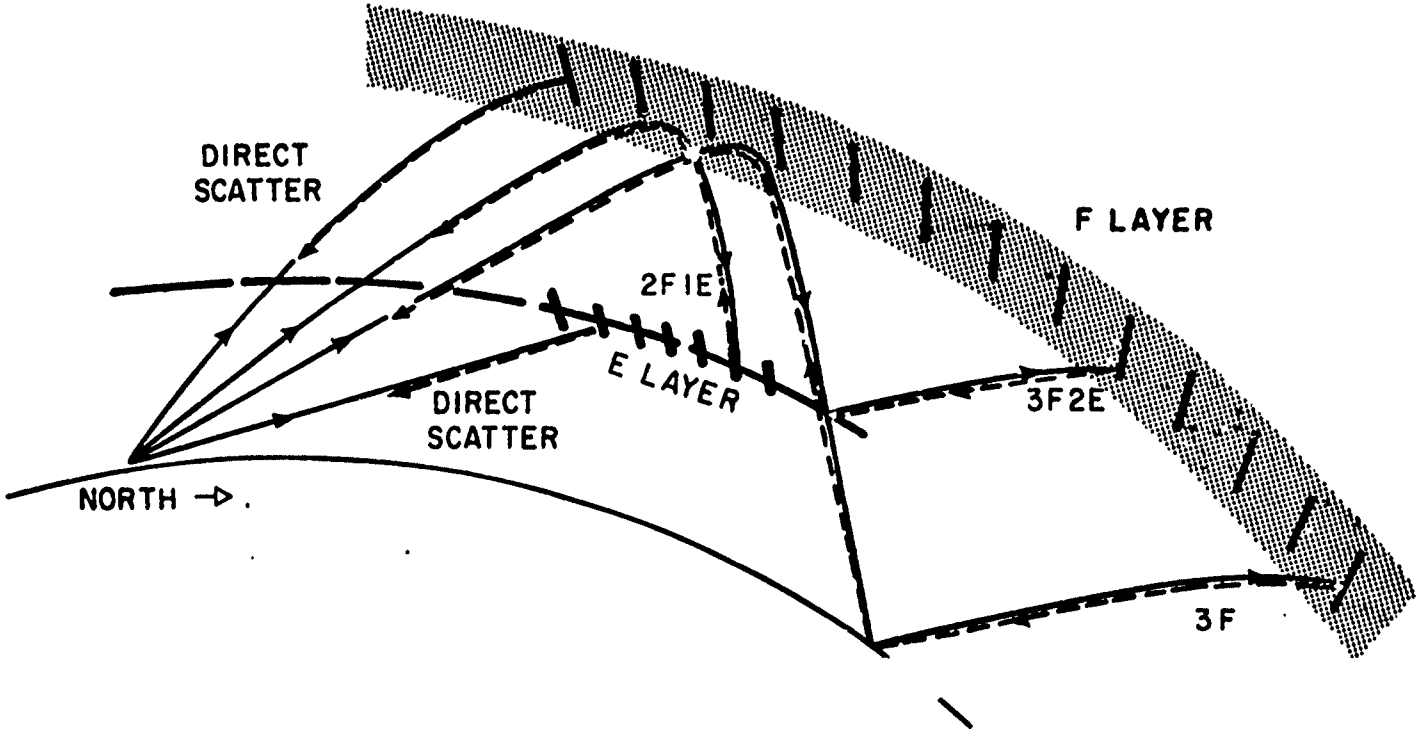

FIG. 15. POSSIBLE MULTI-HOP PROPAGATION MODES AND DIRECT SCATTER FROM FIELD ALIGNED IRREGULARITIES IN THE E AND F LAYERS

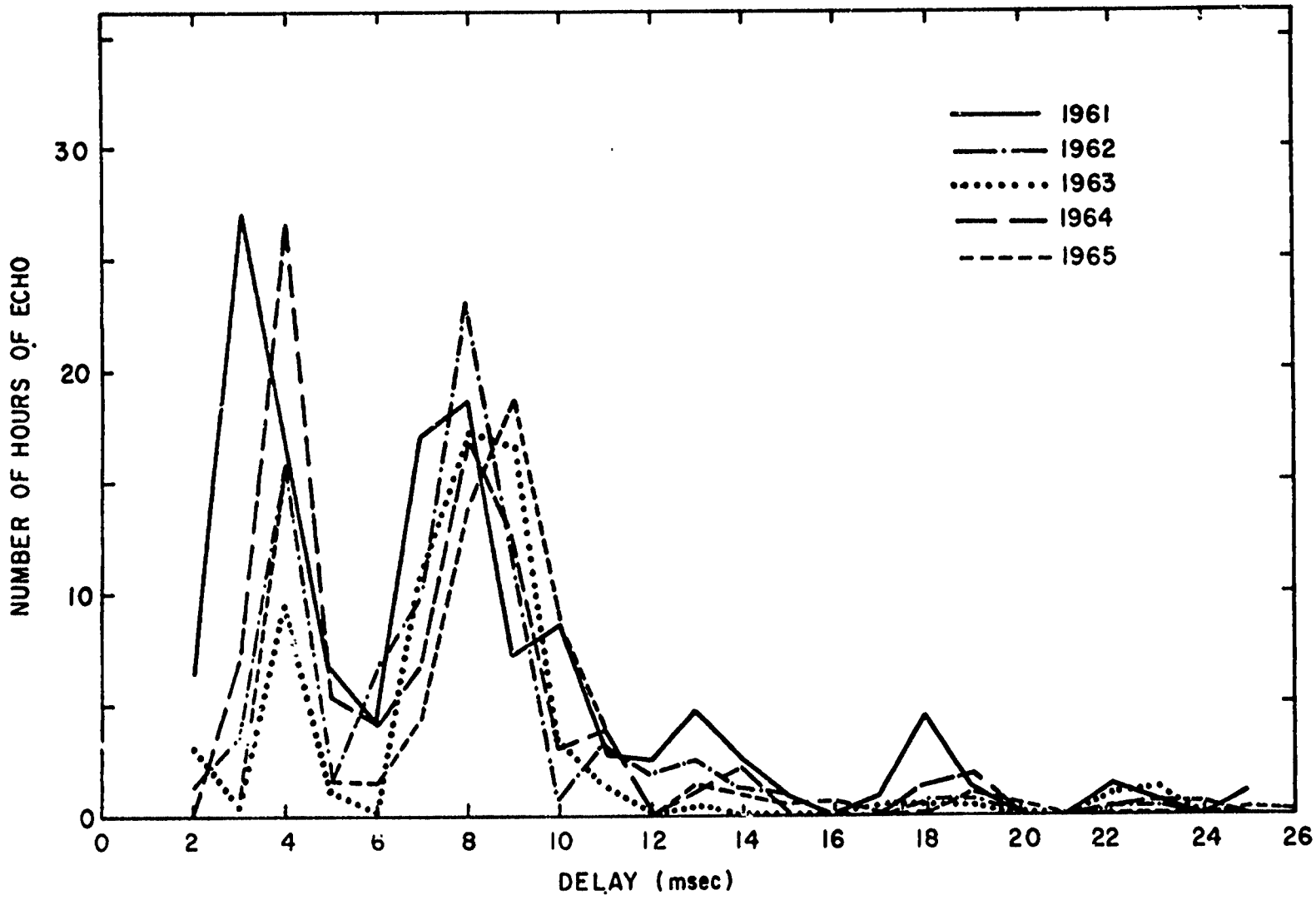

FIG. 14. RANGE DISTRIBUTION OF FAE's DURING THE SPRING SEASON, 1961-1965

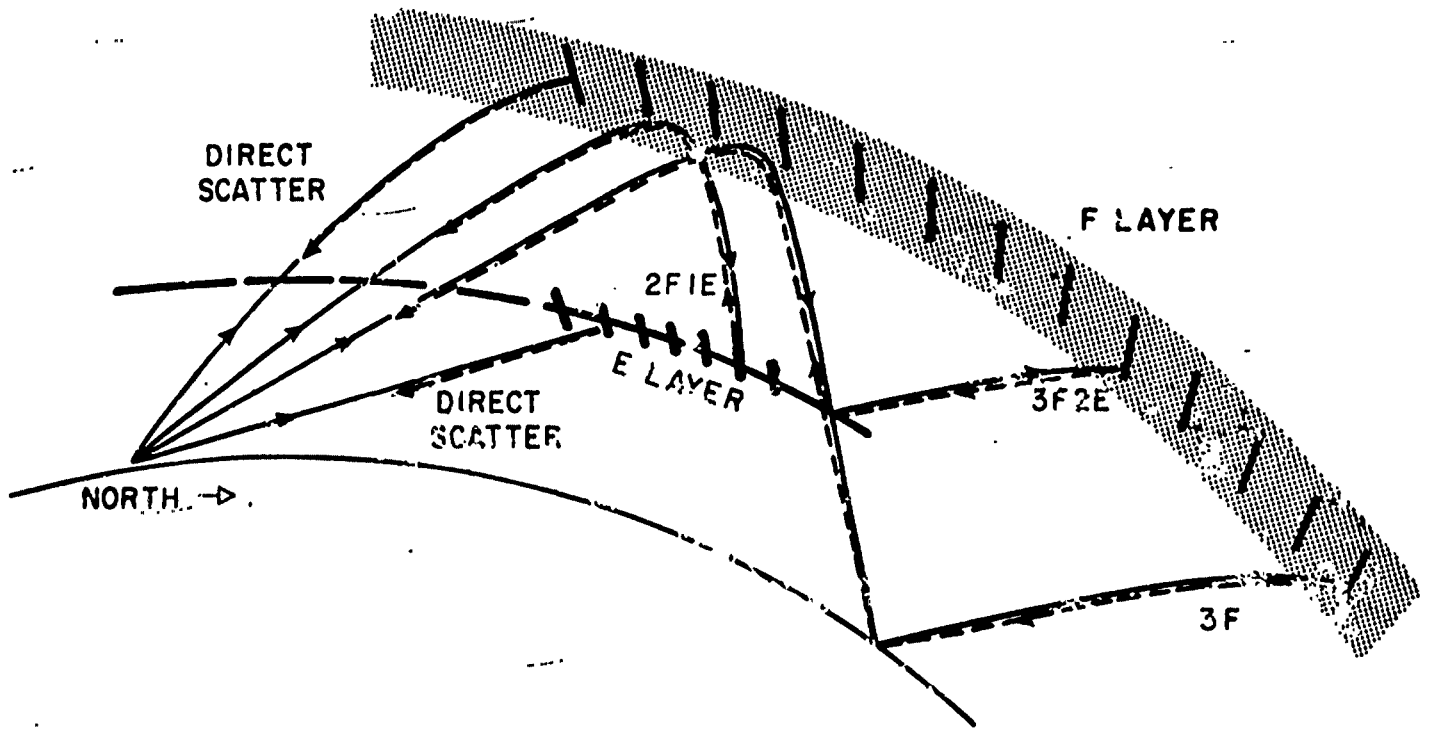

FIG. 15. POSSIBLE MULTI-HOP PROPAGATION MODES AND DIRECT SCATTER FROM FIELD ALIGNED IRREGULARITIES IN THE E AND F LAYERS

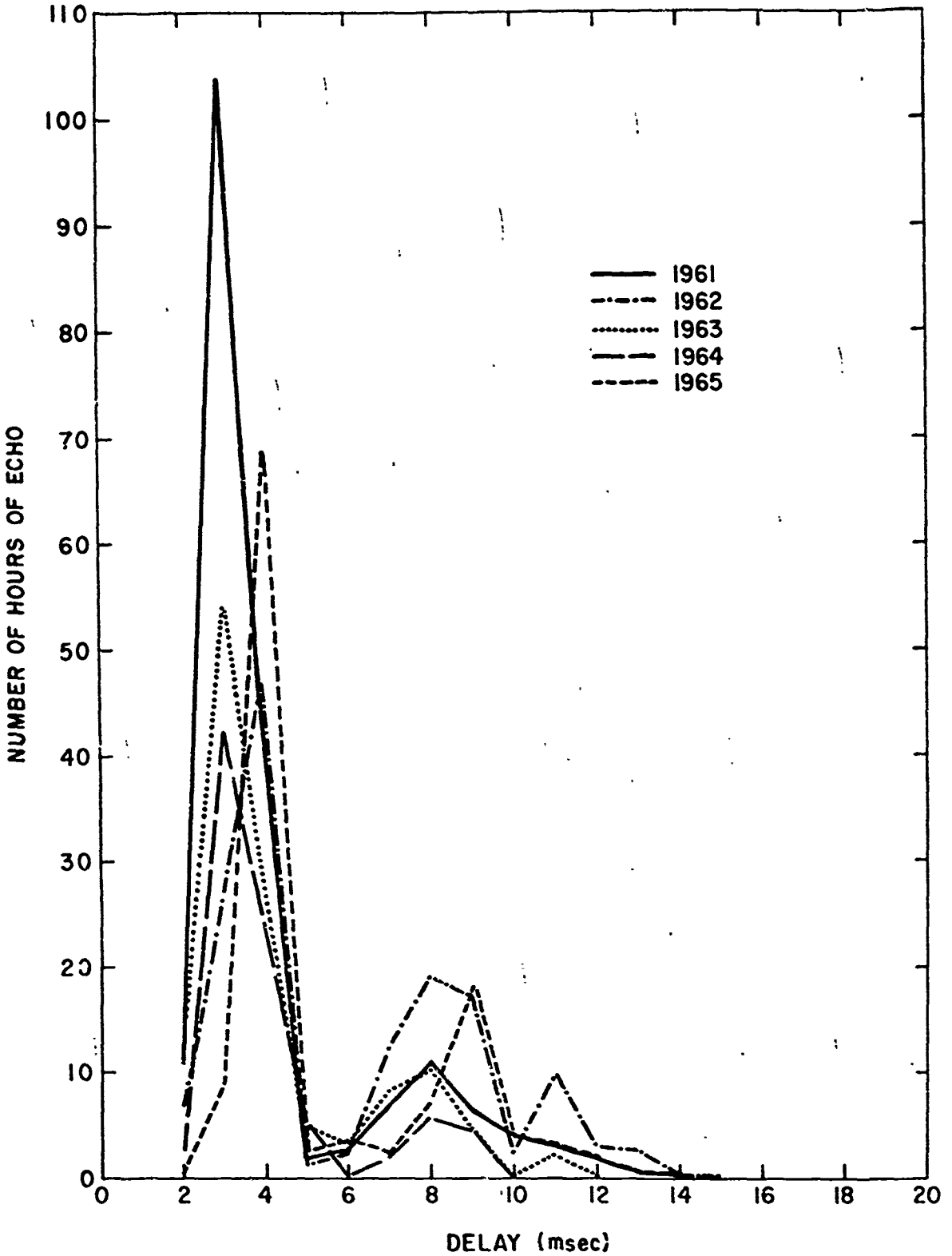

FIG. 16 - RANGE DISTRIBUTION OF FAE's DURING THE SUMMER SEASON, 1961-1965.

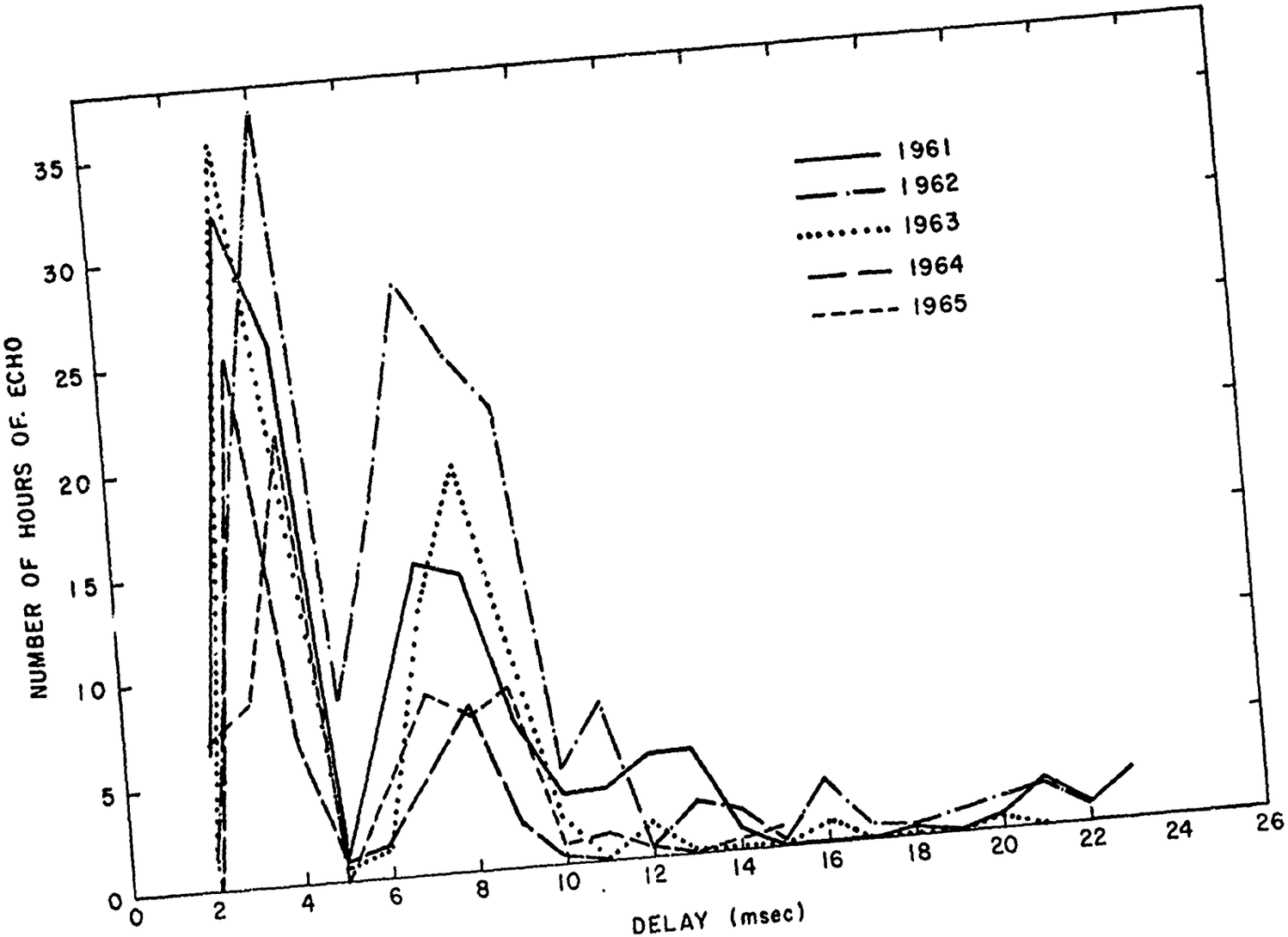

FIG. 17. RANGE DISTRIBUTION OF FAE's DURING THE FALL SEASON, 1961-1965

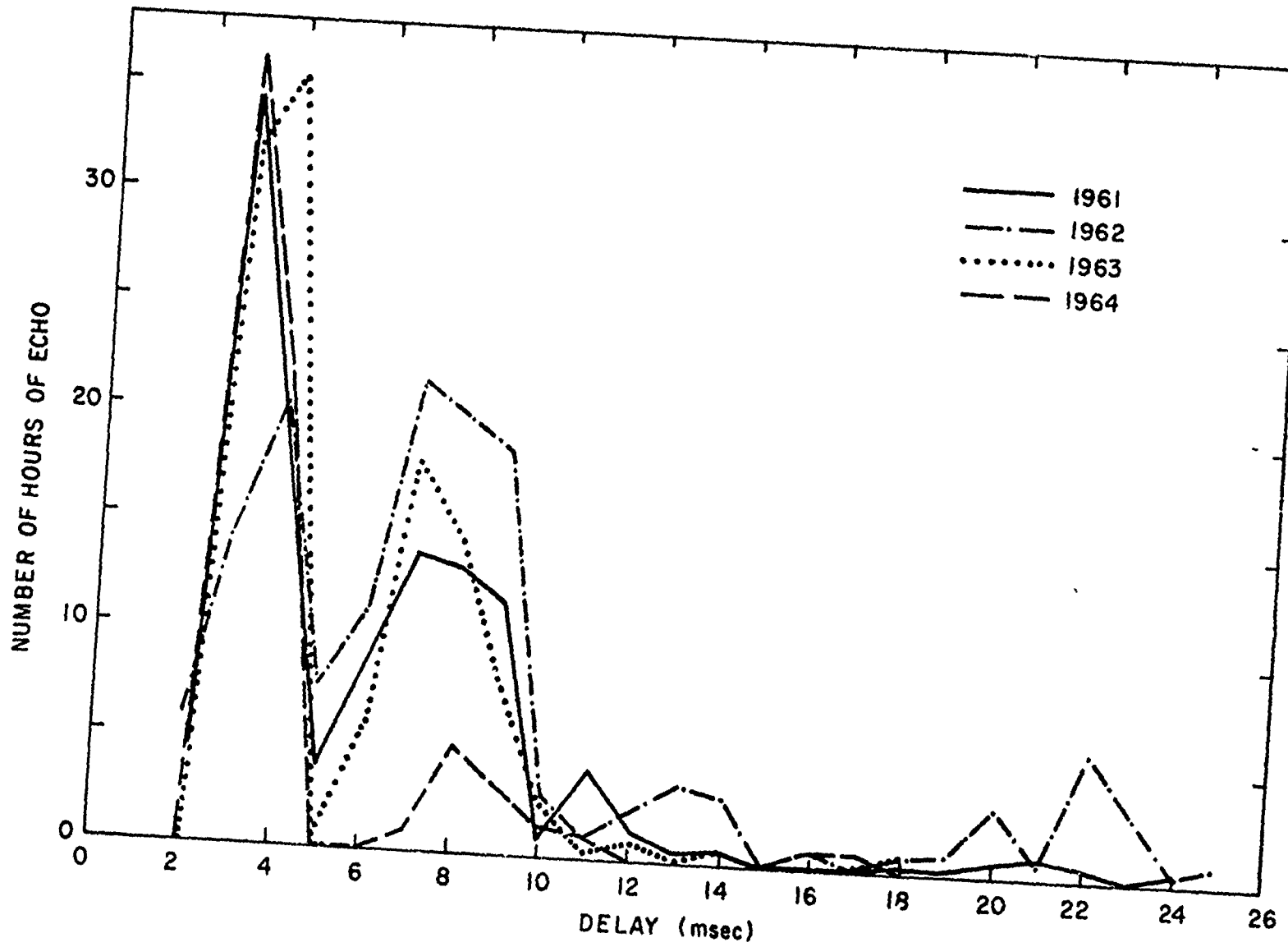

FIG. 18. RANGE DISTRIBUTION OF FAE's DURING THE WINTER SEASON, 1961-1964

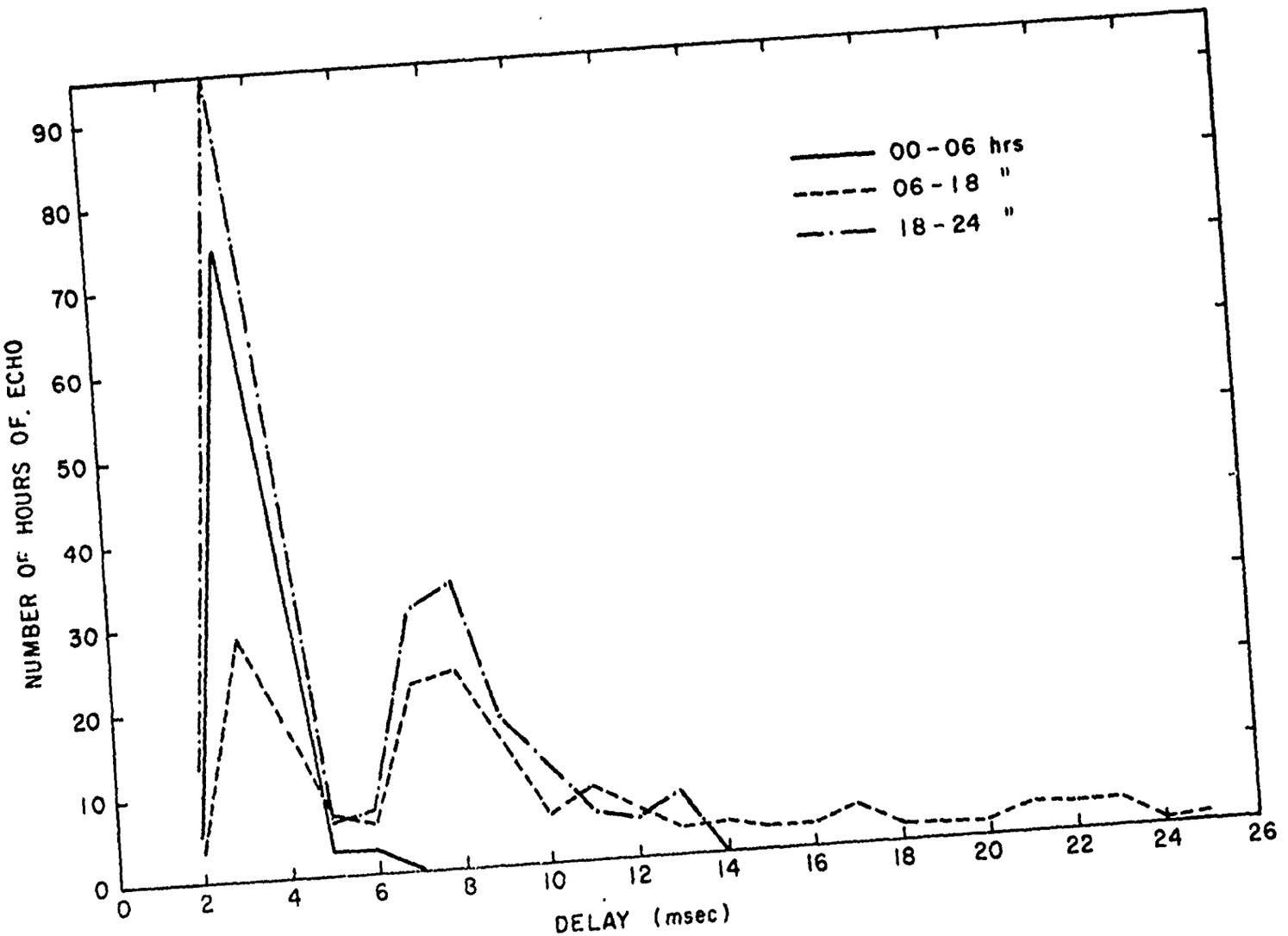

FIG. 19. DIURNAL PATTERN OF THE RANGE DISTRIBUTION OF FAE's FOR 1961

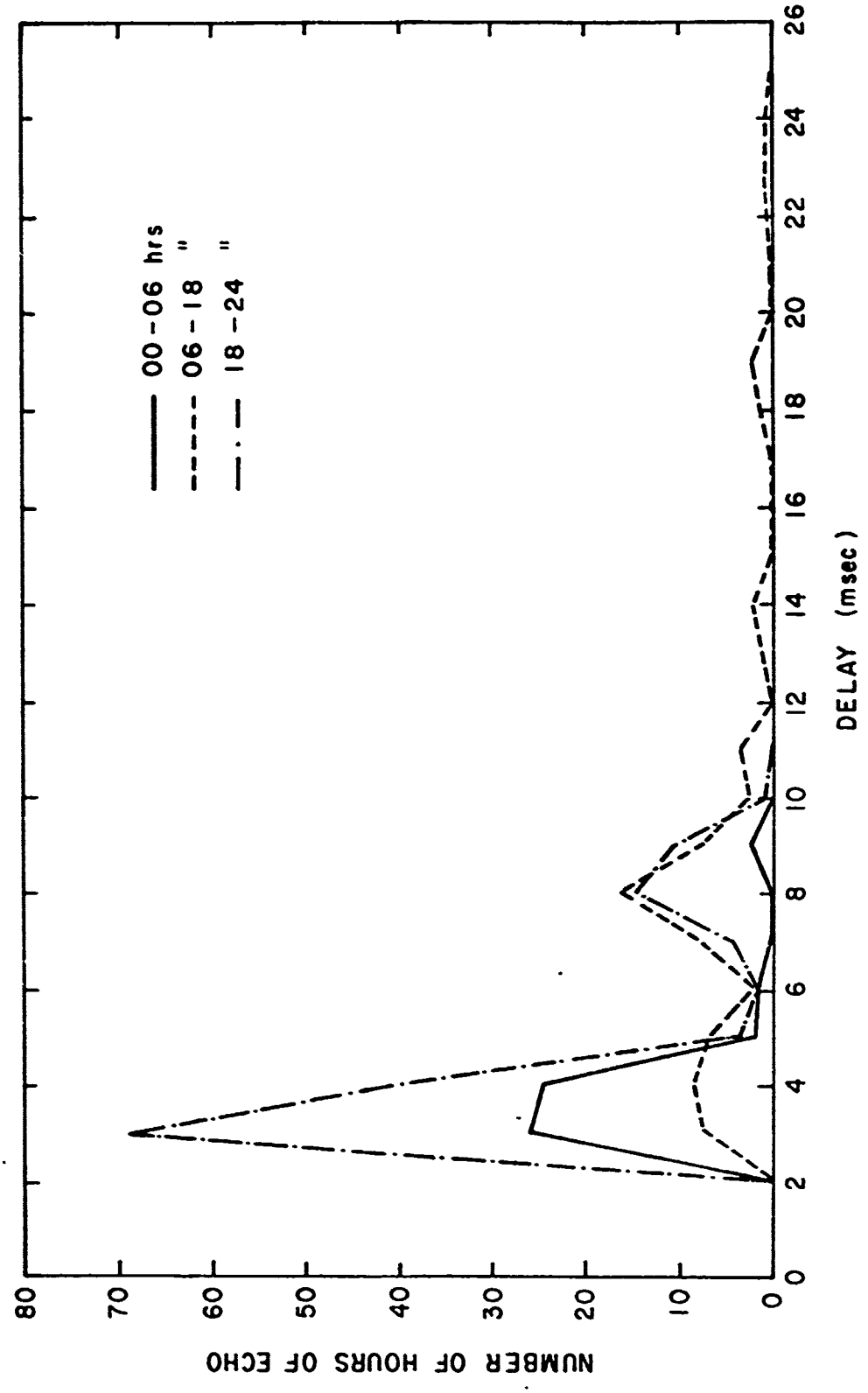

FIG. 20. DIURNAL PATTERN OF THE RANGE DISTRIBUTION OF FAE's FOR 1964

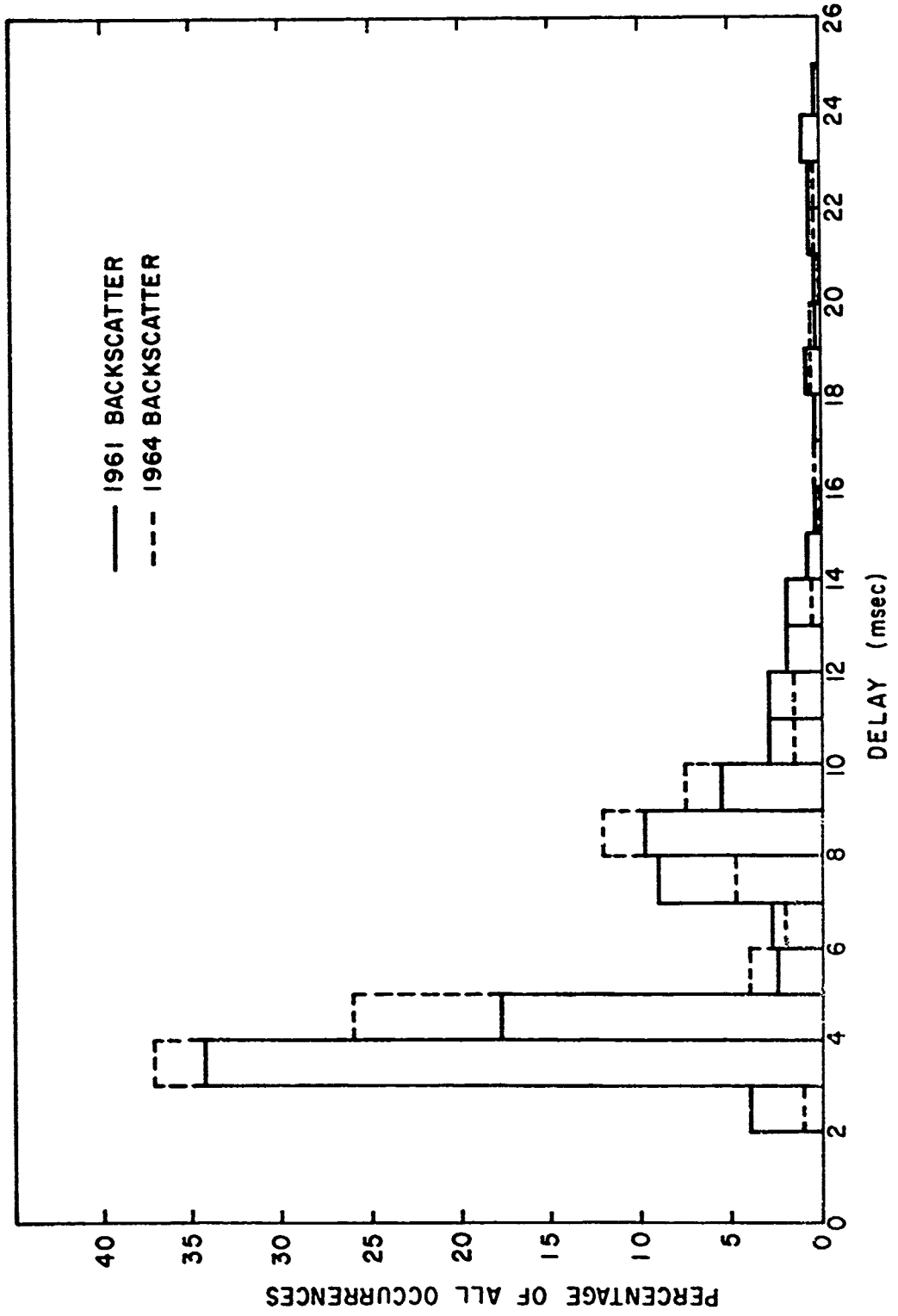

FIG. 21. PERCENTAGE RANGE DISTRIBUTION OF ALL FAE OCCURRENCE FOR 1961 & 1964

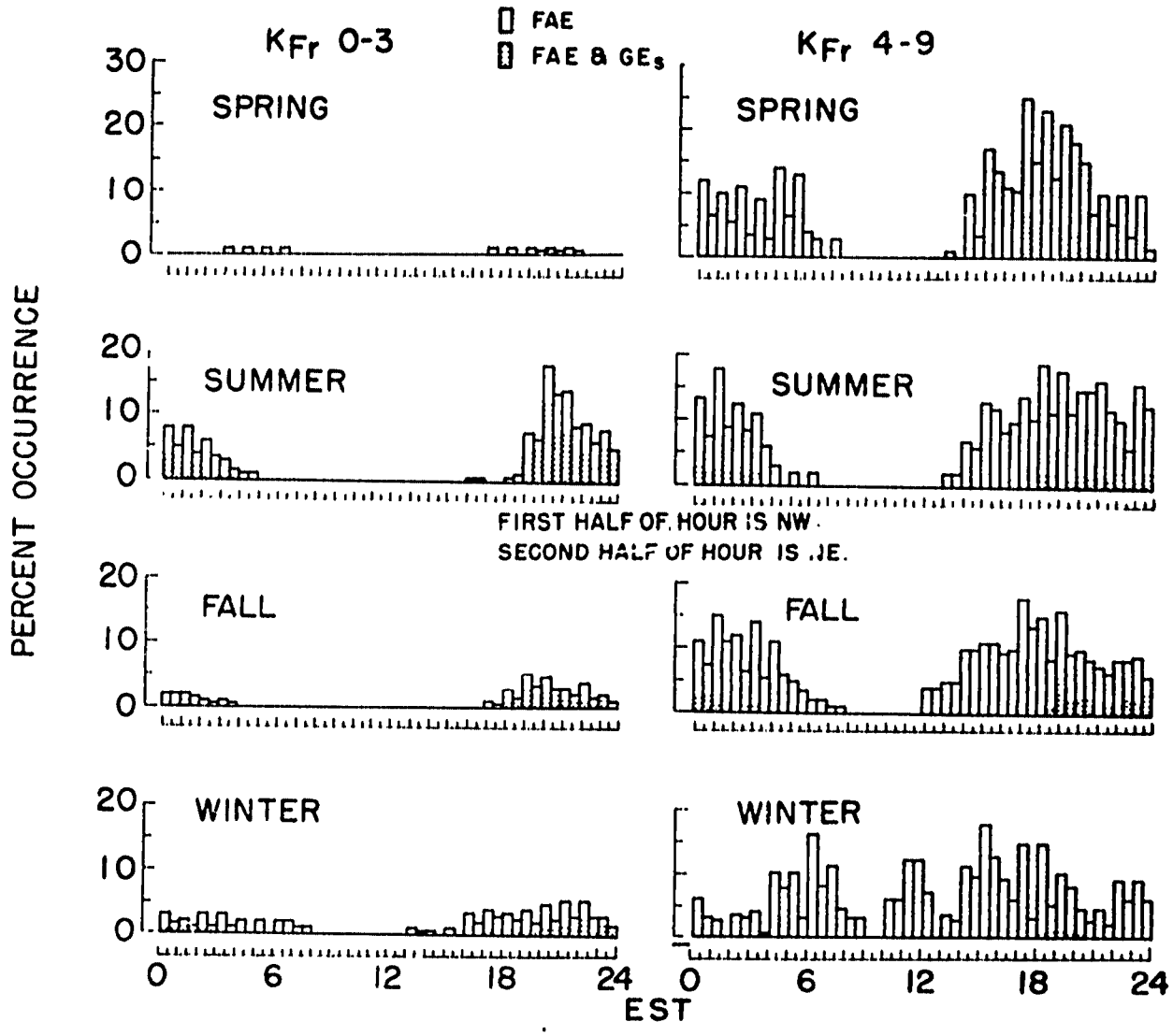

FIG. 22 AVERAGE SEASONAL BEHAVIOR OF FAE (E) DURING MAGNETICALLY QUIET AND DISTURBED PERIODS, 1961-1965

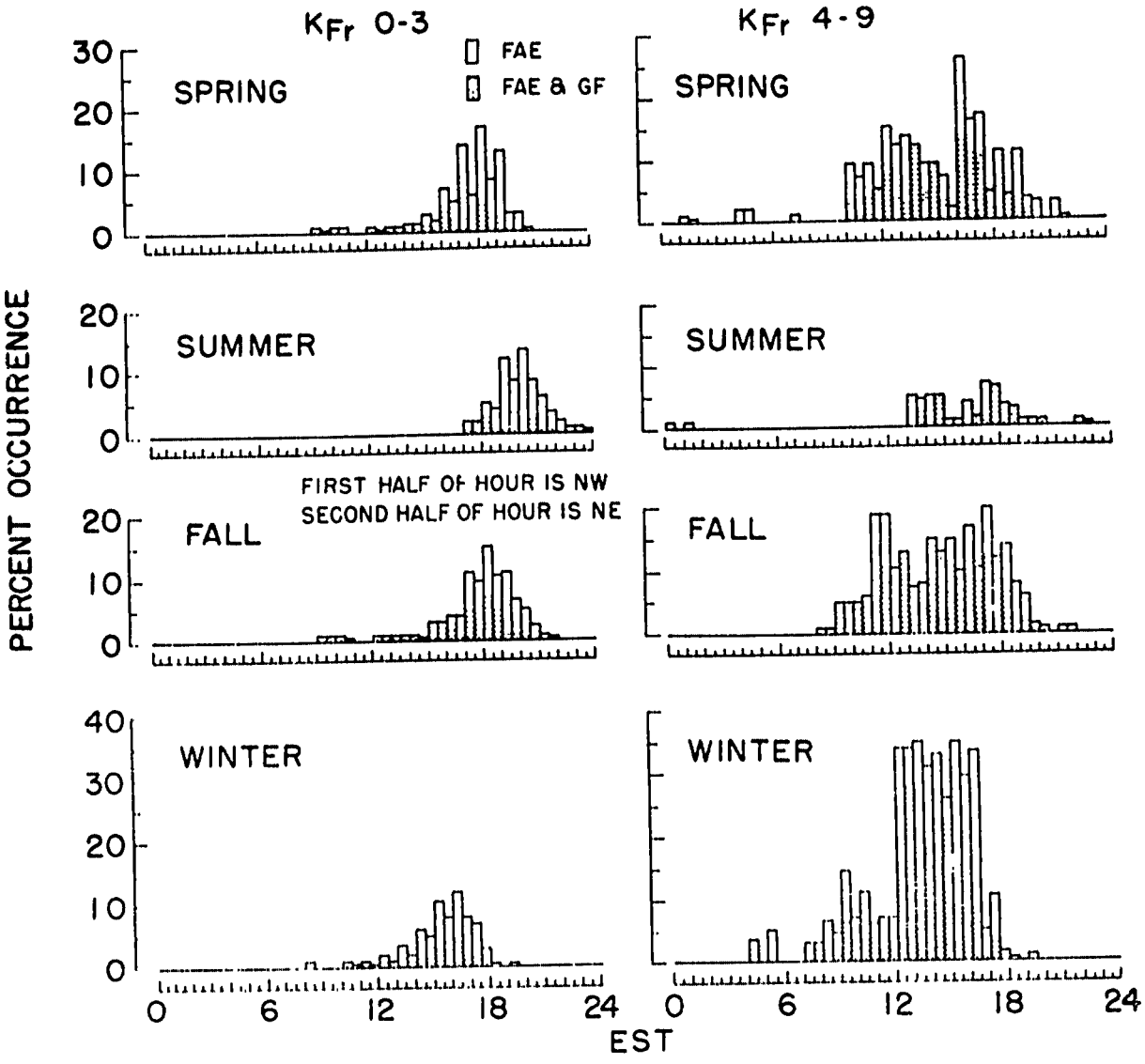

FIG. 23 AVERAGE SEASONAL BEHAVIOR OF FAE (F) DURING MAGNETICALLY QUIET AND DISTURBED PERIODS, 1961-1965

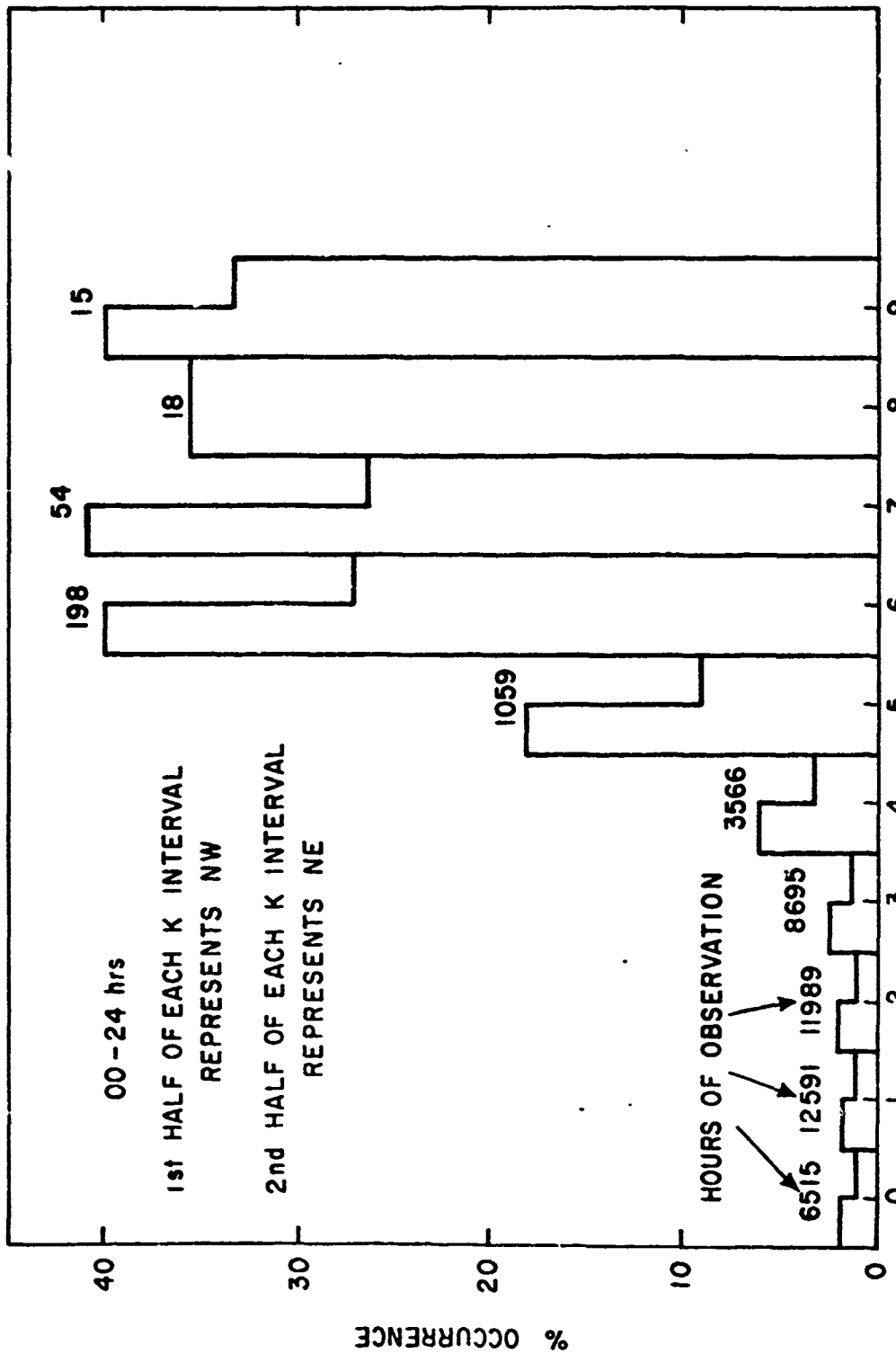

FIG. 24a. FAE (E) AS FUNCTION OF MAGNETIC INDEX K_{FR}

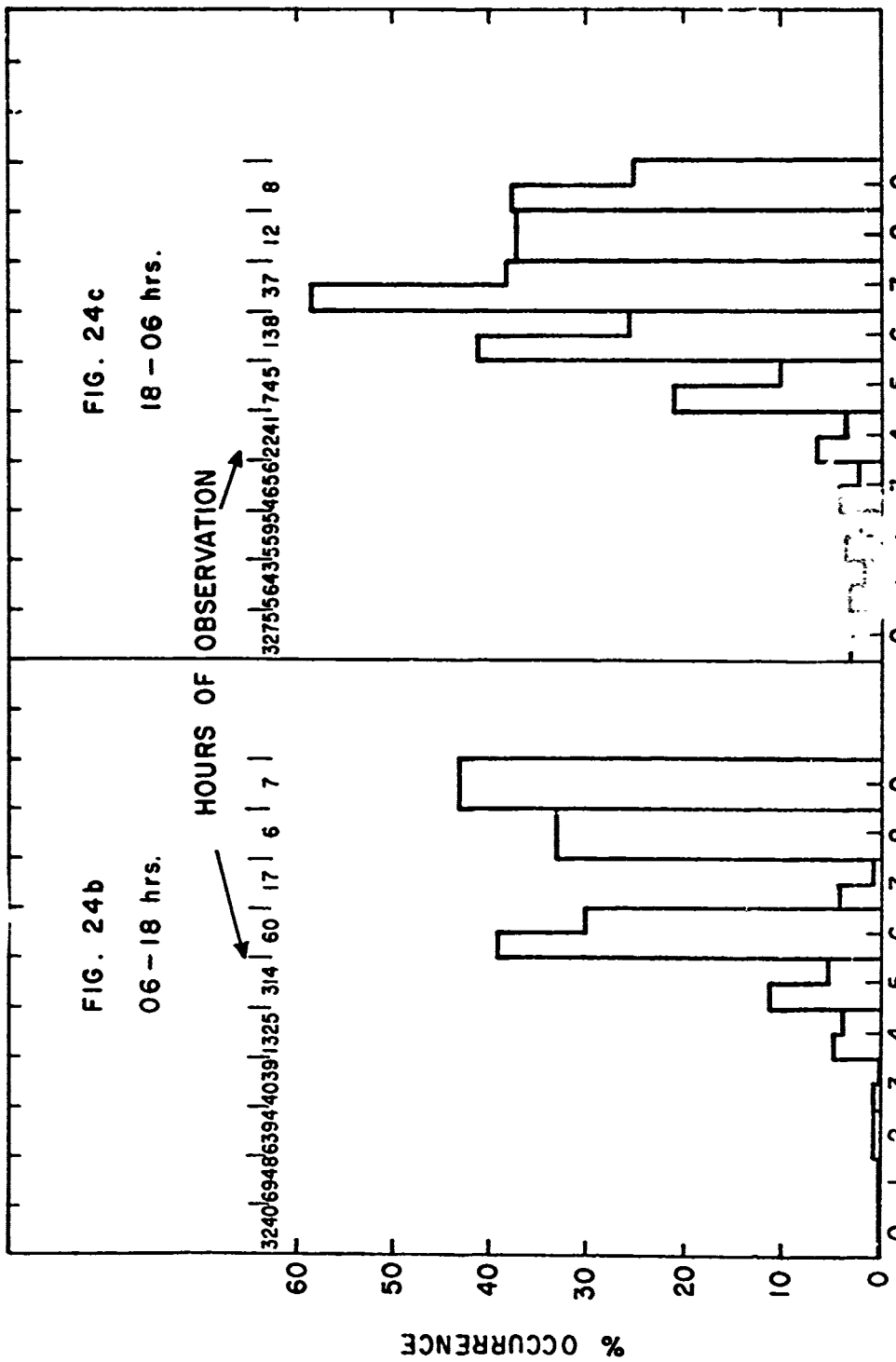

FIG. 24b & 24c. FAE(E) AS A FUNCTION OF MAGNETIC INDEX K_{FR}

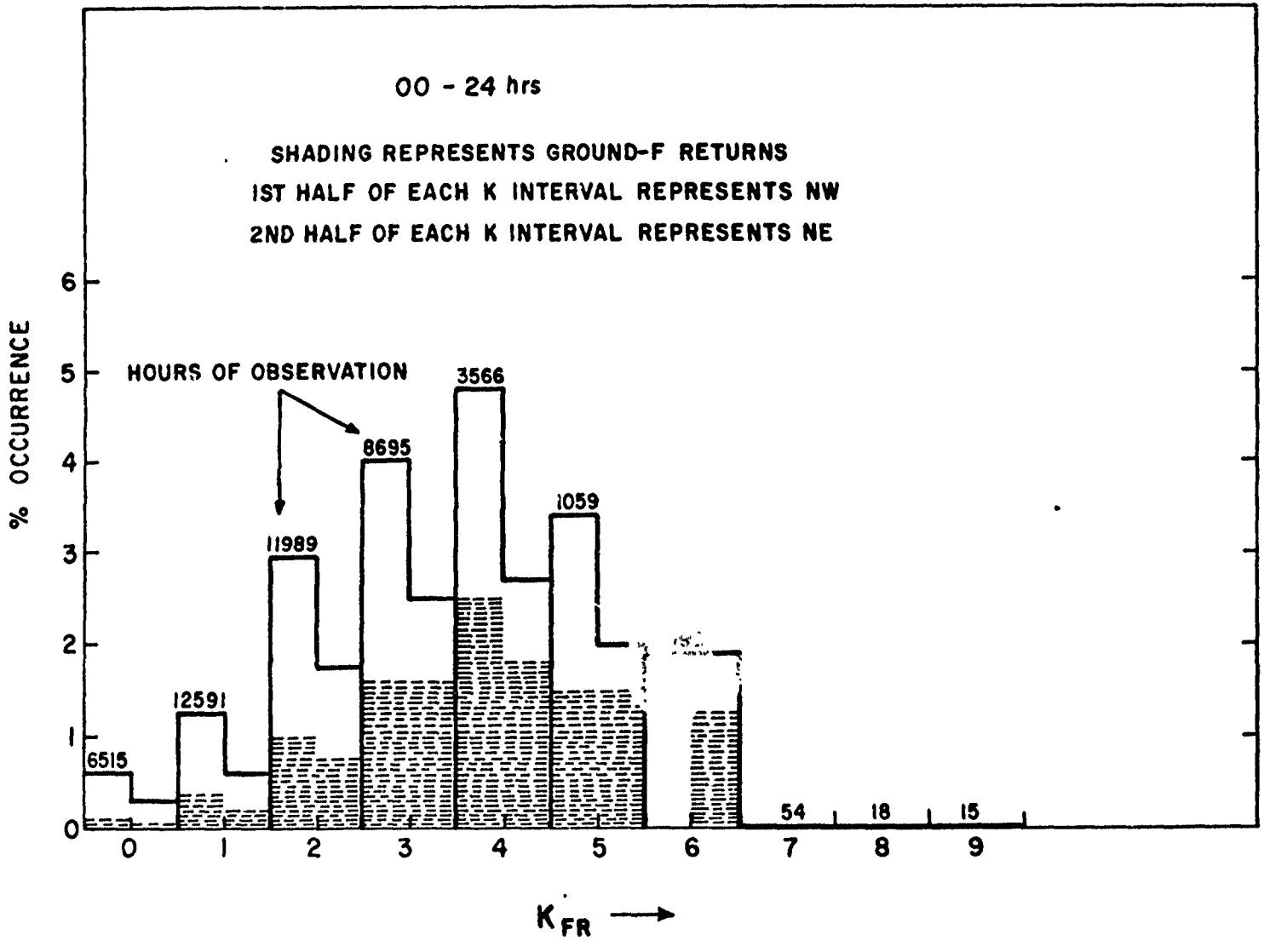

FIG. 25a FAE (F) AS A FUNCTION OF MAGNETIC INDEX K_{FR}

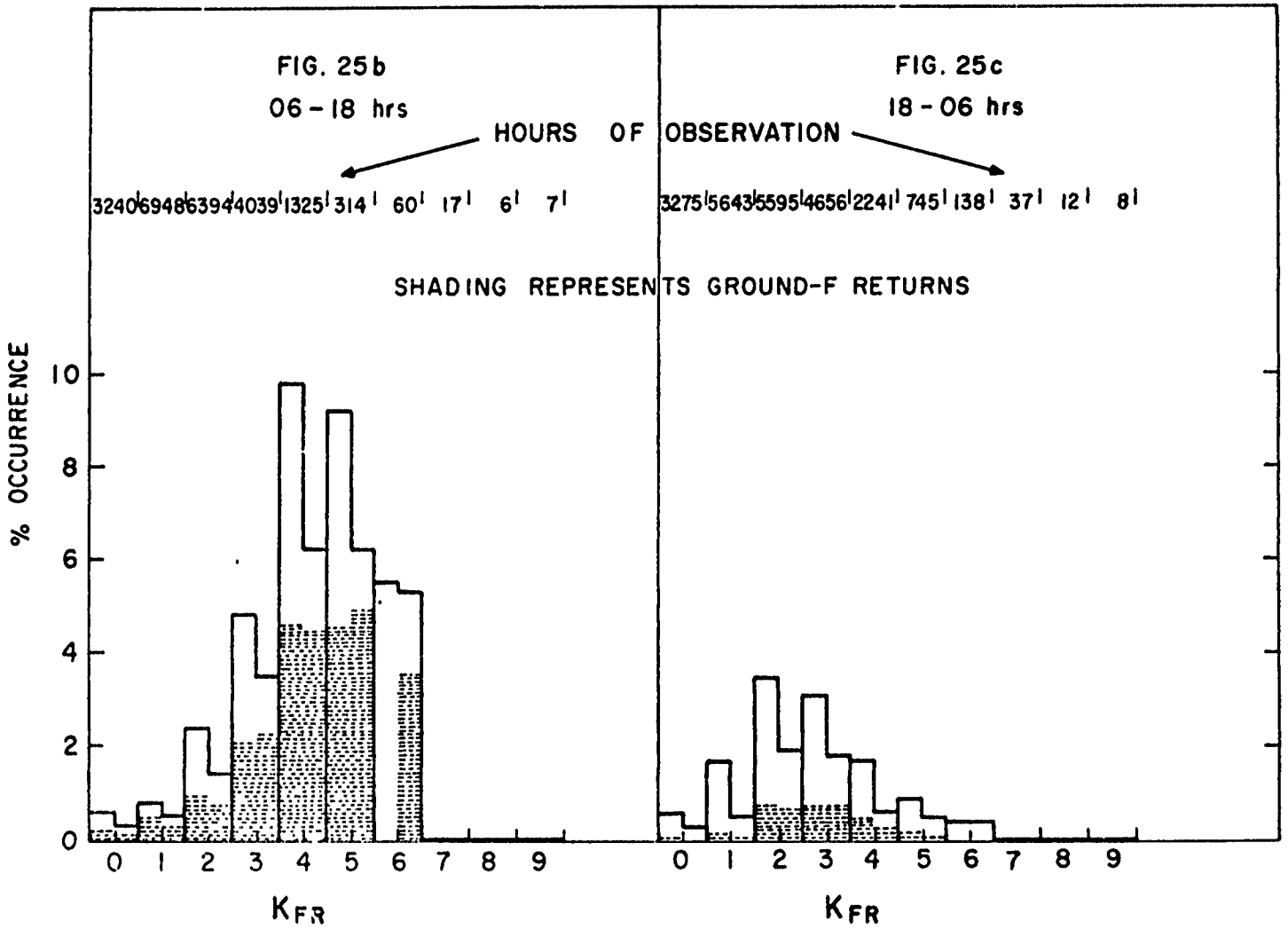

FIG. 25b & 25c. FAE(F) AS A FUNCTION OF MAGNETIC INDEX K_{FR}

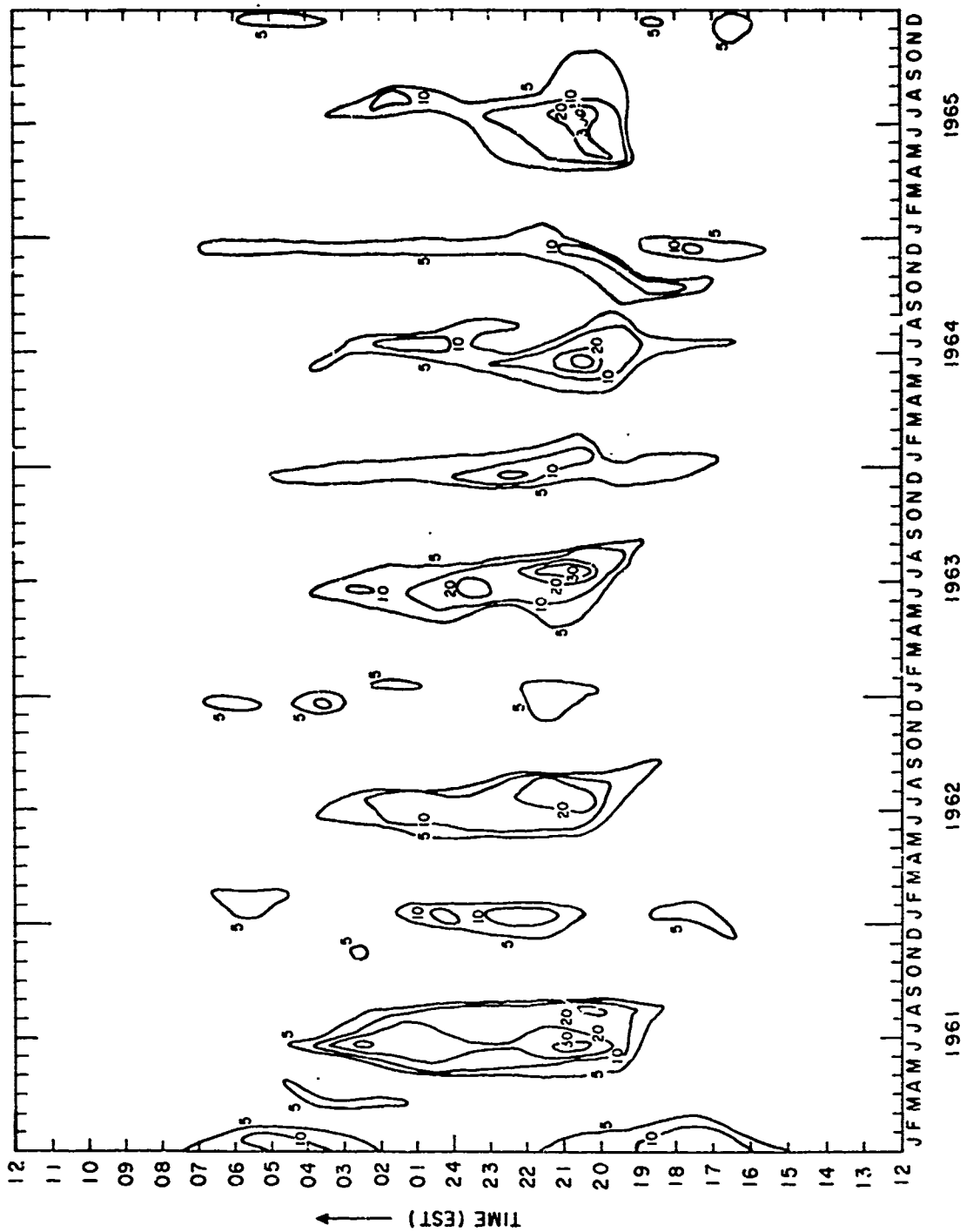

FIG. 26. PERCENTAGE OCCURRENCE CONTOURS OF E-LAYER ECHOES FOR K_{FR} 0-3 FOR 1961-1965

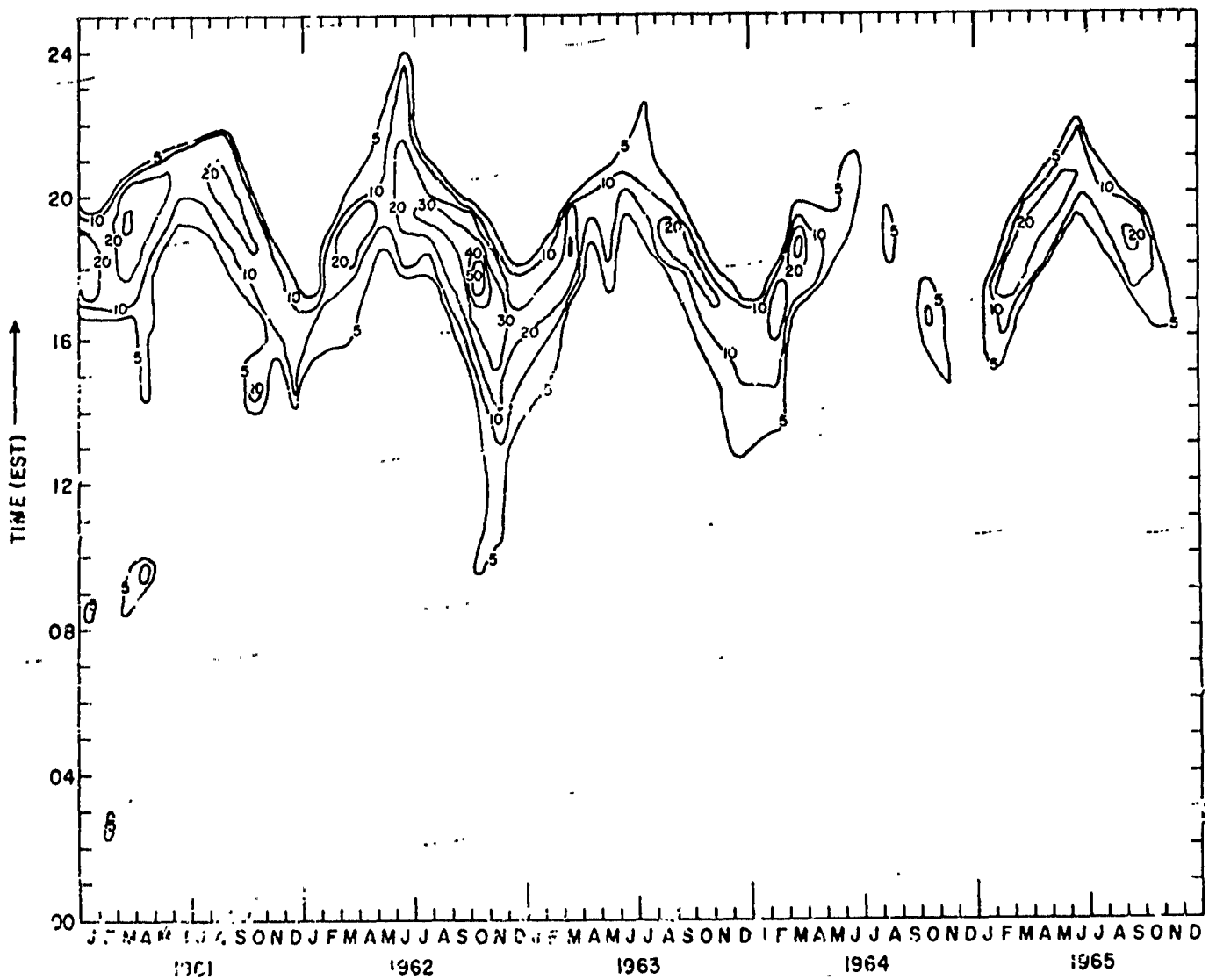

FIG. 27 PERCENTAGE OCCURRENCE CONTOURS OF F-LAYER ECHOES FOR K_{FR} 0-3 FOR 1961-1965

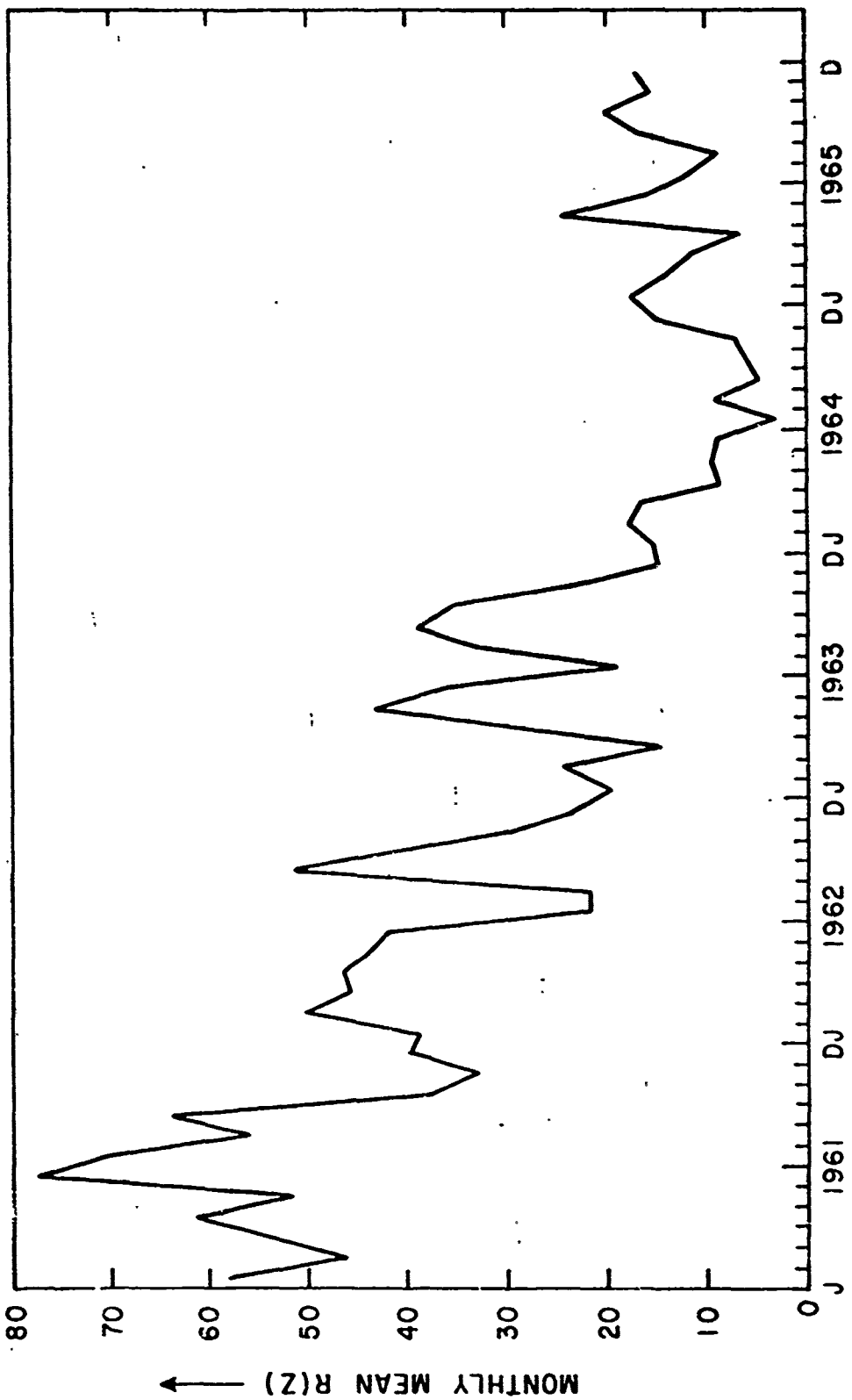

FIG. 28. MEAN ZURICH SUNSPOT NUMBERS FOR 1961-1965

REFERENCES

Aarons, J., H.F. Auroral Backscatter and the Scintillation Boundary in "Radar Propagation in the Arctic", AGARD Symposium, Lindau, Germany, Sept., 1971.

Aarons, J., and R.S. Allen, "Scintillation Boundary during Quiet and Disturbed Magnetic Conditions", J. Geophys. Res., 76, 170, 1971.

Aarons, J., J.P. Mullen, and Sunanda Basu, "Geomagnetic Control of Satellite Scintillations", J. Geophys. Res., 68, 3159, 1963.

Agy, V., A Model for the Study and Prediction of Auroral Effects on HF Radar in "Radar Propagation in the Arctic", AGARD Symposium, Lindau, Germany, Sept., 1971.

Bates, H.H., "The Aspect Sensitivity of Spread-F Irregularities", J. Atmos. Terr. Phys., 33, 111, 1971.

Booker, H.G., "Radar Studies of the Aurora", Physics of the Upper Atmosphere, edited by J. A. Ratcliffe, Academic Press, New York, 1960.

Bowles, K.L., "Radio Wave Scattering in the Ionosphere", Advances in Electronic and Electron Physics, edited by L. Morton, Academic Press, New York, 1964.

Chamberlain, J.W., Physics of the Aurora and Airglow, Academic Press, New York, 1961.

Keck, R.D., and G. L. Hower, "Backscatter Radar Observations at WSU - 1957-1966", Washington State University, College of Engineering, Research Report 68/16-45, Pullman, Washington, 1968.

Leadabrand, R.L., Electromagnetic Measurements of Auroras in "Symposium on Auroras", Palo Alto, California, January, 1964.

Malik, C., and J. Aarons, "A Study of Auroral Echoes at 19.4 Megacycles per Second", J. Geophys. Res., 69, 2731, 1964.

Mendillo, M., M.D. Papagianis, and J.A. Klobuchar, "A Seasonal Effect in the Mid-latitude Slab Thickness Variations During Magnetic Disturbances", J. Atmos. Terr. Phys., 31, 1359, 1969.

Paulikas, G.A., "The Patterns and Sources of High Latitude Particle Precipitation", Rev. Geophys. Space Phys., 9, 659, 1971.